

**Vapor and Liquid ( $p$ - $\rho$ - $T$ - $x$ ) Measurements of Binary Refrigerant  
Blends Containing R-134a, R-1234yf, and R-1234ze(E)\***

**Tara J. Fortin<sup>†</sup>**  
**Mark O. McLinden**

**National Institute of Standards and Technology**  
Material Measurement Laboratory  
Applied Chemicals and Materials Division  
325 Broadway  
Boulder, CO 80305-3328, U.S.A.

Phone: 1-303-497-3522  
Fax: 1-303-497-6682  
E-Mail: [tara.fortin@nist.gov](mailto:tara.fortin@nist.gov)

---

\* Contribution of the National Institute of Standards and Technology. Not subject to Copyright © in the U.S.A.

<sup>†</sup> Corresponding author.

## Abstract

The pressure-density-temperature-composition ( $p$ - $\rho$ - $T$ - $x$ ) data of binary refrigerant mixtures containing R-134a (1,1,1,2-tetrafluoroethane), R-1234yf (2,3,3,3-tetrafluoropropene), and R-1234ze(E) (*trans*-1,3,3,3-tetrafluoropropene) were measured in both the vapor and liquid phases using a two-sinker, magnetic-suspension densimeter. The specific samples in this study comprised two compositions of approximately (0.3/0.7) molar and (0.7/0.3) molar for each of the following three binary refrigerant blends: R-1234yf + R-134a, R-134a + R-1234ze(E), and R-1234yf + R-1234ze(E). Single-phase vapor densities were measured over a temperature range of (253 to 293) K and pressures from approximately (0.04 to 0.5) MPa. Single-phase liquid and supercritical densities were measured over a temperature range of (230 to 400) K and pressures up to 21 MPa; for refrigerant blends containing R-1234yf the maximum pressure was limited to approximately 12 MPa. Overall relative combined, expanded ( $k = 2$ ) uncertainties in density ranged from 0.043% to 0.418%, with an average uncertainty of approximately 0.06%. Here we present measurement results, along with comparisons to available literature data and to default equations of state and mixture models included in REFPROP.

## Keywords

Density; hydrofluorocarbons; hydrofluoroolefins; refrigerant blends

## 1. Introduction

Regulatory efforts, such as the European Union fluorochemical (or “F-Gas”) regulations<sup>1,2</sup> and the Kigali Amendment to the Montreal Protocol,<sup>3</sup> have spurred the search for the next generation of refrigerants with zero ozone depletion potential (ODP) and low global warming potential (GWP). Recent analyses have concluded that only a limited set of candidate fluids show promise as potential replacements for hydrofluorocarbons (HFCs) in low- and medium-temperature refrigeration applications, with hydrofluoroolefins (HFOs) considered the most promising of these.<sup>4-7</sup> The lack of chlorine makes HFOs safe for the ozone layer, while the presence of a double bond results in short atmospheric lifetimes and very low GWPs. For example, the two HFOs measured in this work, R-1234yf (2,3,3,3-tetrafluoropropene) and R-1234ze(E) (*trans*-1,3,3,3-tetrafluoropropene) have estimated atmospheric lifetimes of 12 and 19 days, respectively, translating to GWP<sub>100</sub> of < 1 and 1.<sup>8</sup> In contrast, the HFC R-134a (1,1,1,2-tetrafluoroethane), which was also included in this study, has an estimated lifetime of 14 years and a GWP<sub>100</sub> of 1530.<sup>9,10</sup>

R-134a was introduced in the early 1990s as a replacement for the ozone-destroying chlorofluorocarbon (CFC) R-12 (dichlorodifluoromethane); it was the most common refrigerant used in automobile air conditioners until recent regulations mandated a transition to lower GWP alternatives.<sup>1,2,11,12</sup> R-1234yf was specifically developed as a replacement for R-134a in mobile air conditioners and, despite exhibiting a somewhat lower volumetric cooling capacity, has been successfully adopted by many automobile manufacturers.<sup>13-15</sup> Similarly, R-1234ze(E) has been considered as a potential replacement for HFCs such as R-410A (a 50/50 mass % mixture of R-32 (difluoromethane) and R-125 (pentafluoroethane)) and R-134a in a variety of medium temperature uses, but has demonstrated some limitations that impede its viability as a pure-fluid replacement.<sup>16</sup>

<sup>17</sup> Additionally, both R-1234yf and R-1234ze(E) are mildly flammable with an A2L safety

classification under ANSI/ASHRAE Standard 34.<sup>18</sup> However, the blending of HFOs with more traditional refrigerants, such as the nonflammable R-134a, offers a potential solution to overcome the performance and flammability limitations of the individual pure-fluid refrigerants.

The measurements presented here were part of a larger project aimed at identifying and experimentally demonstrating the performance of several candidate non-flammable refrigerant blends to replace R-134a in military environmental control units.<sup>19</sup> In this work, we report pressure-density-temperature-composition ( $p$ - $\rho$ - $T$ - $x$ ) measurements in the single-phase and supercritical regions for three binary refrigerant blends: R-1234yf + R-134a, R-134a + R-1234ze(E), R-1234yf + R-1234ze(E). Overall, these measurements covered temperatures from approximately (230 to 400) K and pressures up to 21 MPa, and sample compositions were approximately (0.3/0.7) molar and (0.7/0.3) molar for each blend. The project also included comprehensive measurements of vapor-liquid equilibria (VLE)<sup>20</sup> and speed of sound,<sup>21</sup> which together with the density measurements reported here, have been used in the development of new mixture models<sup>22</sup> to replace existing models in REFPROP (Version 10.0) which are based upon estimation schemes or unpublished models.<sup>23, 24</sup> Accurate models based on reliable thermophysical property data are an essential tool for the efficient analysis of the performance of candidate blends in refrigeration applications.

## 2. Materials and Methods

### 2.1 Refrigerant Blends

The three refrigerants used in the blends studied in this work, along with the corresponding chemical formula, CAS number, supplier, and supplier's stated purity, are listed in Table 1. The stated purities of 99.9% or higher were verified by independent gas chromatography-mass

spectrometry (GC-MS) analyses performed at NIST which found no significant impurities. Molecular diagrams for each of the refrigerants are shown in Figure 1.

Prior to mixture preparation, each individual fluid was transferred to stainless steel sample cylinders and degassed. Specifically, the pure components were frozen in liquid nitrogen, the vapor space over the frozen sample was evacuated, and the sample was then thawed; this freeze-pump-thaw cycle was repeated until the residual pressure over the frozen sample was  $< 0.01$  Pa. Additional details of the degassing procedure can be found in Outcalt and Rowane.<sup>20</sup>

The gas-phase mixtures were prepared gravimetrically in aluminum sample cylinders with approximate internal volumes of 10 or 13 L depending on the pressure of a given mixture. The sample cylinders were loaded to pressures below the dew-point pressure at  $T = 293.15$  K. Additionally, during testing, the cylinders were heated continuously to  $T > 313$  K to ensure that only single-phase vapor was present. The sample masses were determined via a double substitution weighing scheme<sup>25</sup> that utilized a nearly identical “tare” or reference cylinder as the main substitution mass. Potential errors from a non-linear balance response and air buoyancy effects are minimized using this method. Additional details regarding the gravimetric preparation of gas-phase mixtures can be found in Richter and McLinden.<sup>26</sup> Table 2 shows the final compositions for each of the six measured samples and total sample volumes. Two different balances were employed in the preparation of these samples. Specifically, the 10 L samples utilized a balance with a 10 kg maximum capacity and a 0.1 mg resolution, while the 13.4 L samples utilized a balance with a 41 kg maximum capacity and a 1 mg resolution.

As a result of the double substitution weighing scheme employed here, the standard uncertainty in the composition due to the gravimetric preparation alone was estimated at 0.00005 mole fraction. However, additional sources of uncertainty in composition must be considered.

These include sample purity, external cylinder contamination, cylinder expansion upon filling, sorption effects,<sup>26</sup> and uncertainties associated with sample loading; they are discussed in greater detail in Section 3.2.

## 2.2 Apparatus Description

A custom-built two-sinker densimeter was utilized for the measurements reported in this work. This type of instrument provides an absolute determination of density via application of the Archimedes, or buoyancy, principle and the use of two sinkers improves the accuracy.<sup>27, 28</sup> The densimeter has previously been described in detail by McLinden and Lösch-Will;<sup>29</sup> only a brief description is provided here.

A high-precision balance was used to separately weigh two sinkers with nearly identical masses and surface areas, but drastically different volumes, while the sinkers were immersed in a fluid of unknown density. The fluid density,  $\rho$ , is given by

$$\rho = \frac{(m_1 - m_2) - (W_1 - W_2)}{(V_1 - V_2)}, \quad (1)$$

where  $m$  is the sinker mass,  $V$  is the sinker volume,  $W$  is the balance reading, and the subscripts refer to the two sinkers. In this work, the sinkers were made of tantalum ( $m = 60.094633$  g and  $V = 3.60872$  cm<sup>3</sup>) and titanium ( $m = 60.075386$  g and  $V = 13.315284$  cm<sup>3</sup>). The gravity and buoyancy forces on the sinkers are transmitted to the balance via the utilization of a magnetic suspension coupling, thus isolating the fluid sample from the balance. With the two-sinker densimeter, the systematic errors in the weighing and from other sources approximately cancel, resulting in greater accuracy relative to other buoyancy techniques.

For each density determination, the balance was calibrated via the use of two calibration masses (referred to as “cal” and “tare”) that were weighed by placing them directly on the balance pan; these additional weighings also provided information needed to correct for magnetic effects.<sup>30</sup>

<sup>31</sup> The two sinker weighings and two calibration mass weighings yielded a set of four equations that were solved to produce a balance calibration factor,  $\alpha$ , and a parameter describing the efficiency of the magnetic suspension coupling,  $\phi$ . The fluid density could then be calculated as

$$\rho = \left\{ \left[ (m_1 - m_2) - \frac{(W_1 - W_2)}{\alpha\phi} \right] / (V_1 - V_2) \right\} - \rho_0, \quad (2)$$

where  $\rho_0$  is the density when the sinkers are weighed in vacuum, which accounts for small changes in sinker masses that occur over time. Eq 2 compensates for the magnetic effects of both the apparatus and the fluid being measured. The difference of the value of  $\phi$  from 1 indicates the magnitude of the force transmission.<sup>30, 31</sup> In this work,  $\phi$  varied from 1.000003 to 1.000004 in vacuum and from 0.999965 to 1.000027 during refrigerant blend measurements.

The densimeter was thermostated with a multi-layer, vacuum-insulated thermostat. An “inner shield” made of copper, with heaters at the top and side, surrounded the measuring cell. This was surrounded by an additional “outer shield” whose temperature was maintained at a constant temperature approximately 1 K below that of the measuring cell via use of heaters at the top and sides and a fluid cooling channel at the top. Subambient temperatures were achieved via use of a chiller circulating ethanol through the fluid channel on the outer shield.

The measuring cell temperature was measured with a 25  $\Omega$  standard platinum resistance thermometer (SPRT) and an AC resistance bridge referenced to a thermostated standard resistor. For the work reported here, the cell temperature was constant to within 5 mK. Pressure was measured using one of three vibrating-quartz-crystal type pressure transducers with full-scale pressure ranges of 2.8 MPa, 13.8 MPa, or 69 MPa. To minimize the effects of temperature variations, all three transducers and the pressure manifold were maintained at  $T = (313.15 \pm 0.20)$  K.

## 2.3 Experimental Procedures

Vapor-phase densities were measured along isotherms at approximate temperatures of 253.15 K, 263.15 K, 273.15 K, 283.15 K, and 293.15 K. For each isotherm, approximately (36 to 106) kPa of fresh sample was manually introduced into the evacuated measuring cell, after which, two pneumatic valves piped in series were automatically cycled to inject additional sample for subsequent pressure increases. An initial equilibration period of 30–60 min was allowed at each pressure, after which, four replicate density determinations were made.

For liquid and supercritical phase densities, a combination of measurements along isochores and isotherms was carried out over temperatures from approximately (230 to 400) K. For each refrigerant blend, liquid sample was loaded by cooling the evacuated measuring cell and condensing gas-phase sample from the sample bottle into the cell (see Section S1 of Supporting Information for additional information regarding sample loading). Once filled, the valve between the sample manifold and the measuring cell was closed, and the pressure subsequently increased by raising the cell temperature in steps along a pseudoisochore. To avoid potential polymerization reactions, the maximum pressure was limited to approximately 12 MPa for refrigerant blends containing R-1234yf.<sup>32</sup> At each new temperature and pressure, an additional equilibration time of 30–60 min was allowed, after which, four replicate density determinations were carried out. Once the maximum pressure along a pseudoisochore was reached, the pressure was then decreased by venting a portion of the sample into a waste bottle. Measurements continued in this manner along an isotherm to a minimum pressure of approximately 1 MPa or slightly above the bubble-point pressure, whichever was higher. Temperatures were then increased along the next, lower-density pseudoisochore. By following this procedure, we were able to avoid any possible contamination

from the use of a pump or compressor and to minimize the number of manual sample-handling steps.

Before and after all testing, and between each measured refrigerant blend, the measurement cell and all filling and pressure lines were evacuated for a minimum of 36 h to ensure the complete removal of the previously measured sample and to check the zero of the pressure transducers and the  $\rho_0$  of the apparatus (eq 2). In this work, the  $\rho_0$  varied by less than  $0.0010 \text{ kg}\cdot\text{m}^{-3}$ .

### 3. Results and Discussion

#### 3.1 Measurement Results

The measured ( $p$ - $\rho$ - $T$ - $x$ ) state points for the six samples studied in this work are plotted as density vs temperature in Figure 2. R-1234yf + R-134a is shown in Figures 2a ( $x_1 = 0.33634$  molar) and 2b ( $x_1 = 0.64709$  molar), R-134a + R-1234ze(E) is shown in Figures 2c ( $x_1 = 0.33250$  molar) and 2d ( $x_1 = 0.66356$  molar), and R-1234yf + R-1234ze(E) is shown in Figures 2e ( $x_1 = 0.33584$  molar) and 2f ( $x_1 = 0.66660$  molar). In all cases, the experimental temperatures have been averaged over the 12 minutes required to complete a single density determination and all replicate density determinations are shown. For reference, the data shown in Figure 2 are also presented in Tables S1–S6 of the Supporting Information. Also included in Figure 2 are the corresponding phase boundaries (red line) and the critical points (red asterisk). Points below the phase boundary line are vapor-phase measurements, while those above and to the right are liquid and supercritical phase measurements.

Averages of the replicate measurements made at each ( $T, p$ ) state point have been tabulated in Tables 3–8, along with the associated standard uncertainty in pressure ( $u(p)$ ) and the relative combined, expanded ( $k = 2$ ) state-point uncertainty in density ( $100 \cdot (U(\rho)/\rho)$ ). (All of the replicate

data are given in the Supporting Information.) The uncertainty analysis is discussed in detail in Section 3.2. Finally, Tables 3–8 include relative deviations from the default models included in REFPROP (Version 10.0)<sup>24</sup> ( $\Delta\rho$ ) which were calculated as

$$\Delta\rho = 100 \cdot \left( \frac{\rho_{\text{exp}} - \rho_{\text{REF}}}{\rho_{\text{REF}}} \right), \quad (3)$$

where  $\rho_{\text{exp}}$  is the experimentally determined density and  $\rho_{\text{REF}}$  is the density calculated using REFPROP.<sup>24</sup> The observed deviations relative to REFPROP<sup>24</sup> will be discussed in detail in Section 3.3.

### 3.2 Measurement Uncertainty

Only a brief discussion of the measurement uncertainty associated with density data collected with the two-sinker densimeter is given here. For a more detailed treatment, the reader is directed to earlier works.<sup>29, 33, 34</sup> The main sources of uncertainty were the sinker volumes ( $V_1$ ,  $V_2$ ), the weighings of the sinkers and calibration masses ( $W_1$ ,  $W_2$ ,  $W_{\text{cal}}$ ,  $W_{\text{tare}}$ ), the masses of the sinkers and calibration masses ( $m_1$ ,  $m_2$ ,  $m_{\text{cal}}$ ,  $m_{\text{tare}}$ ), the apparatus zero  $\rho_0$ , and the variance in replicate balance readings. The standard uncertainty in the density measurement can be expressed as

$$u(\rho) = 10^{-6} \rho \cdot \sqrt{\{28\}^2 + \{0.38(T - 293)\}^2 + \{0.63p\}^2} + 0.0010, \quad (4)$$

where the radical term represents the uncertainty in the sinker volumes and the final, constant term incorporates all other uncertainties. In eq 4,  $u(\rho)$  and  $\rho$  are in units of  $\text{kg}\cdot\text{m}^{-3}$ ,  $T$  is in K, and  $p$  is in MPa. The standard uncertainty in density as expressed by eq 4 does not take into consideration the effects of temperature, pressure, or mixture composition. These additional contributions are discussed next.

The SPRT used to measure the temperature was calibrated on ITS-90 from 234 K to 505 K using multiple fixed-point cells. The uncertainty in the fixed point cells, combined with the drift in both the SPRT and the standard transistor, and the presence of any temperature gradients, result in an estimated 3 mK standard uncertainty in temperature. The instrument's three pressure transducers were calibrated with gas-operated piston gages. The resulting standard uncertainty in pressure was estimated to be  $(20 \times 10^{-6} \cdot p + 0.03 \text{ kPa})$  and  $(26 \times 10^{-6} \cdot p + 1.0 \text{ kPa})$  for the vapor-phase and liquid-phase measurements, respectively; these estimates include the uncertainty in the pressure transducers, as well as contributions from the hydrostatic head correction. As was the case with the balance readings, the standard deviations in measured temperature and pressure observed over a complete density determination were added to the above uncertainty estimates.

With mixtures, the uncertainty in the composition contributes significantly to the overall uncertainty in density. The uncertainty analysis presented here follows the example discussed in detail by Richter and McLinden.<sup>26</sup> In this work, in addition to the previously discussed uncertainty associated with the gravimetric preparation of the gas mixture, the uncertainty associated with adsorption of sample (onto the sample cylinder, filling lines, measuring cell, etc.) was estimated to contribute approximately  $0.0052 \text{ g} \cdot \text{mol}^{-1}$ .<sup>26</sup> The uncertainty in sample purity was estimated to have an additional contribution of  $(0.0002 \cdot \rho) \text{ kg} \cdot \text{m}^{-3}$ . The resulting absolute combined, standard uncertainty in density resulting from the uncertainty in composition was estimated to be  $(0.0004\text{--}0.2915) \text{ kg} \cdot \text{m}^{-3}$  (see the accompanying Supporting Information).

When comparing  $(p, \rho, T, x)$  measurements to a model, all uncertainties are typically combined into a single so-called expanded ( $k = 2$ ) state-point uncertainty for density using the following expression

$$U(\rho) = 2 \cdot \sqrt{[u(\rho)]^2 + \left[ \left( \frac{\partial \rho}{\partial p} \right)_T u(p) \right]^2 + \left[ \left( \frac{\partial \rho}{\partial T} \right)_p u(T) \right]^2 + [u_\rho(x)]^2}, \quad (5)$$

where the radical terms represent the standard uncertainties in density (calculated via eq 4), pressure, temperature, and composition, all expressed in units of  $\text{kg} \cdot \text{m}^{-3}$ . The results are converted to relative combined, expanded state-point uncertainties and are reported in Tables 3–8. Overall, the observed uncertainties ranged from 0.043% to 0.418%, with an average uncertainty of approximately 0.06%. In general, the largest uncertainties were associated with vapor-phase measurements.

### 3.3 Data Comparisons

Existing mixture models included in REFPROP<sup>24</sup> employ pure component Helmholtz energy empirical multi-parameter equations of state (EoS) along with binary interaction parameters and mixing rules. The density measurements reported here, combined with the other comprehensive thermophysical property measurements completed during this project, have been used to improve upon existing mixture models. The results of those modeling efforts have been published by Bell.<sup>22</sup> In this work, reported comparisons instead focus on the default mixture models included in REFPROP (Version 10.0)<sup>24</sup> in an effort to provide additional context for the modeling results. Relative deviations have been calculated according to eq 3 and the results tabulated in Tables 3–8. The comparison results have also been plotted as percent deviation vs temperature (a), pressure (b), and density (c) and are shown in Figure 3 for R-1234yf + R-134a, in Figure 4 for R-134a + R-1234ze(E), and in Figure 5 for R-1234yf + R-1234ze(E). In each graph, the  $x_1 \approx 0.3$  molar composition data are represented by circles and the  $x_1 \approx 0.7$  molar composition data are represented by squares. The experimental data are also distinguished by marker color; specifically, vapor-phase data are shown in black, liquid-phase data are shown in red, and data above the

corresponding critical temperature are shown in blue. Finally, smoothed curves representing the combined, expanded uncertainty for each binary mixture are also shown for reference (dashed lines) and graph insets show vapor-phase data in greater detail where needed.

For the three refrigerant mixtures discussed here, the default mixture models included in REFPROP (Version 10.0)<sup>24</sup> employed the EoS published by Tillner-Roth and Baehr<sup>35</sup> for R-134a, Richter et al.<sup>32</sup> for R-1234yf, and Thol and Lemmon<sup>36</sup> for R-1234ze(E). For R-1234yf + R-134a, R-134a + R-1234ze(E), as well as R-1234yf + R-1234ze(E), corresponding binary interaction parameters were derived from unpublished work.<sup>23</sup>

To aid in our comparisons, the average absolute deviation (AAD) and the maximum absolute deviation (MAD) have been calculated as

$$\text{AAD} = 100 \cdot \left\{ \frac{1}{N} \sum_{i=0}^N \left| \frac{\rho_{\text{exp},i} - \rho_{\text{REF},i}}{\rho_{\text{REF},i}} \right| \right\}, \quad (6)$$

and

$$\text{MAD} = \max \left\{ 100 \cdot \left| \frac{\rho_{\text{exp},i} - \rho_{\text{REF},i}}{\rho_{\text{REF},i}} \right| \right\} \quad (7)$$

where  $\rho_{\text{exp},i}$  is the  $i^{\text{th}}$  experimental density value,  $\rho_{\text{REF},i}$  is the  $i^{\text{th}}$  density value calculated using REFPROP,<sup>24</sup> and  $N$  is the total number of data points. The overall AAD and MAD for the three binary mixtures are listed in Table 9. The R-134a + R-1234ze(E) mixture shows the best agreement with current mixture models with an AAD of 0.137%, while the R-1234yf + R-1234ze(E) mixture shows the worst with an AAD of 0.412%.

The primary observations to be made about the data presented in Figures 3–5 are as follows. First, the experimental densities are generally higher than those calculated with REFPROP;<sup>24</sup> although a significant fraction of the liquid and vapor data for the R-1234yf + R-134a mixture exhibit lower densities, while all of the measured vapor densities for the R-134a + R-1234ze(E) mixture are lower than calculated values. Second, unsurprisingly, the worst deviations are

observed for near-supercritical and supercritical state points. More specifically, overall, the vapor-phase AADs range from 0.009% to 0.196%, while the ranges are from 0.130% to 0.401% for the liquid phase, and from 0.331% to 1.498% for supercritical state points. The overall largest MAD are 0.217% for vapor, 1.991% for liquid, and 3.774% for supercritical state points. Third, the observed deviations exceed estimated experimental uncertainties for all liquid and supercritical measurements. In contrast, the vapor measurements exhibit deviations that are largely within overall average experimental uncertainties, which range from 0.058% to 0.065%, and almost entirely within vapor-specific uncertainties, which range from 0.046% to 0.246%. Finally, distinct behavior is observed in the vapor and liquid phases for the two compositions of the R-1234yf + R-134a mixture. Specifically, the deviations for the  $x_1 = 0.33634$  molar composition blend are lower than the  $x_1 = 0.64709$  molar composition blend with vapor AADs of 0.015% and 0.196%, respectively, and liquid AADs of 0.130% and 0.233%, respectively.

Comparisons have also been made to available literature data for the R-1234yf + R-134a, the R-134a + R-1234ze(E), and the R-1234yf + R-1234ze(E) mixtures. Once again, deviations relative to the corresponding default REFPROP<sup>24</sup> models were calculated according to eq 3; the results are plotted as a function of temperature in Figure 6 and as a function of composition in Figure 7. The experimental results from this work are also shown. As with Figures 3–5, the two compositions for each blend are distinguished by separate markers, but no distinction is made between the different physical states in Figures 6 and 7. No distinction is made for differences in composition or physical state for any of the literature data; however, the range of compositions for which data are available is made clear in Figure 7. Additionally, the light orange shaded region shown in each graph of Figure 6 designates the range of corresponding critical temperatures. Select regions of data have been enlarged and shown in graph insets when needed for clarity. Finally, the

overall AAD and MAD have been determined for each literature data set; the results are documented in Table 9.

Several observations can be made from the data shown in Table 9 and Figures 6 and 7. The primary thing to notice is that the results from this work are generally in agreement with existing literature data, with our results showing slightly better agreement with default mixing models than all but one data set, that of Yotsumoto et al.<sup>37</sup> for R-1234yf + R-134a, which has an AAD of 0.057% compared to an AAD of 0.240% for this work. The one striking outlier is the Higashi data set for R-1234yf + R-1234ze(E), which has an AAD of 3.450% and an MAD of 23.030%. However, large deviations are not unexpected given that the measurements in question were chiefly made near the critical point (see Figure 6c). The second thing to note is that, as was observed in this work, the literature densities for R-1234yf + R-1234ze(E) are generally higher than the values calculated with REFPROP.<sup>24</sup> For R-134a + R-1234ze(E), the Al Ghafri et al.<sup>38</sup> densities are generally higher, while those of Zhang et al.<sup>39</sup> are all lower. For R-1234yf + R-134a, all of the literature data sets show a mix of higher and lower densities relative to calculated values. Finally, the measurement results from this work nicely complement existing data sets for R-1234yf + R-134a in terms of temperature, pressure, density, and composition, but for R-134a + R-1234ze(E) and R-1234yf + R-1234ze(E) they represent a significant expansion of the available literature data, particularly in terms of pressure and density.

Although the comparisons discussed herein have focused on the default mixture models included in REFPROP (Version 10.0),<sup>24</sup> it is worth noting that we have also compared our experimental results with the updated mixture models reported by Bell.<sup>22</sup> These new mixture models incorporate new binary interaction parameters<sup>22</sup> developed with the aid of the full suite of thermophysical property measurements conducted as part of this project,<sup>20,21</sup> as well as a new EoS

for R-1234yf.<sup>40</sup> Table 10 lists the resulting AADs and MADs for reference; results of comparisons with literature data are discussed by Bell.<sup>22</sup> In all cases, the new mixture models show a significant improvement over the default models.

## 4. Conclusions

In this work, the ( $p$ - $\rho$ - $T$ - $x$ ) measurement results for the refrigerant blends R-1234yf + R-134a, R-134a + R-1234ze(E), and R-1234yf + R-1234ze(E) have been presented. The measurements were conducted using a two-sinker densimeter with a magnetic suspension coupling and covered temperatures from (230 to 400) K and pressures up to approximately 21 MPa. These experimental conditions covered vapor, liquid, and supercritical state points, with densities that ranged from approximately (2 to 1403) kg·m<sup>-3</sup>. The resulting AADs for comparisons with default mixture models included in REFPROP (Version 10.0)<sup>24</sup> were, in increasing order, 0.137% for R-134a + R-1234ze(E), 0.240% for R-1234yf + R-134a, and 0.412% for R-1234yf + R-1234ze(E). For all three refrigerant mixtures, comparisons with available literature data<sup>37-39, 41-43</sup> show generally good agreement; for comparison, AADs for available literature data relative to default mixture models ranged from 0.057% to 3.450%. In all cases, supercritical state points showed the largest deviations. The accurate density data presented here complement existing data sets for R-1234yf + R-134a, and significantly expand the available literature data for both R-134a + R-1234ze(E) and R-1234yf + R-1234ze(E). As a result, these data have been integral to the development of improved mixture models that will be made available in future versions of REFPROP.<sup>22, 24</sup>

## Acknowledgments

The authors thank our NIST colleagues Dr. Megan Harries and Dr. Jason Widegren for providing compositional analysis of the pure fluids utilized in the preparation of the measured mixtures, Dr. Aaron Rowane for assistance in mixture preparation, and Dr. Ian Bell for providing relevant available literature data. This work was supported by the Strategic Environmental Research and Development Program; Project WP19-1385: WP-2740 Follow-On: Low-GWP Alternative Refrigerant Blends for HFC-134a.

### **Associated Content**

Replicate density determinations at each of the  $(T, p)$  state points measured in this study are included in Tables S1–S6 of the Supporting Information file, which is available free of charge at <https://pubs.acs.org/doi/10.1021/acs.jced.xxx>. The replicate data presented in Tables S1–S6, as well as the averaged data presented in Tables 3–8, are available for download as tab-delimited text files at <https://doi.org/10.18434/mds2-2780>.

## References

- (1) Directive 2006/40/EC of the European Parliament and of the Council of 17 May 2006 Relating to Emissions from Air-Conditioning Systems in Motor Vehicles and Amending Council Directive 70/156/EEC. *Official J. Eur. Union* **2006**, L 161, 14.6.2006, 12.
- (2) Regulation (EC) No 842/2006 of the European Parliament and of the Council of 17 May 2006 on Certain Fluorinated Greenhouse Gases. *Official J. Eur. Union* **2006**, L161, 14.6.2006, 1.
- (3) *Kigali Amendment to the Montreal Protocol on Substances that Deplete the Ozone Layer*; United Nations: New York, NY, USA, 2016.
- (4) Bell, I. H.; Domanski, P. A.; McLinden, M. O.; Linteris, G. T. The Hunt for Nonflammable Refrigerant Blends to Replace R-134a. *Int. J. Refrig.* **2019**, *104*, 484-495.
- (5) Domanski, P. A.; Brignoli, R.; Brown, J. S.; Kazakov, A. F.; McLinden, M. O. Low-GWP Refrigerants for Medium and High-Pressure Applications. *Int. J. Refrig.* **2017**, *84*, 198-209.
- (6) McLinden, M. O.; Brown, J. S.; Brignoli, R.; Kazakov, A. F.; Domanski, P. A. Limited Options for Low-Global-Warming-Potential Refrigerants. *Nat. Commun.* **2017**, *8*, 14476.
- (7) McLinden, M. O.; Kazakov, A. F.; Brown, J. S.; Domanski, P. A. A Thermodynamic Analysis of Refrigerants: Possibilities and Tradeoffs for Low-GWP Refrigerants. *Int. J. Refrig.* **2014**, *38*, 80-92.
- (8) Hodnebrog, Ø.; Aamaas, B.; Fuglestedt, J. S.; Marston, G.; Myhre, G.; Nielsen, C. J.; Sandstad, M.; Shine, K. P.; Wallington, T. J. Updated Global Warming Potentials and Radiative Efficiencies of Halocarbons and Other Weak Atmospheric Absorbers. *Rev. Geophys.* **2020**, *58*, e2019RG000691.
- (9) *Inventory of U.S. Greenhouse Gas Emissions and Sinks: 1990-2020*; EPA 430-R-22-003; U.S. Environmental Protection Agency: Washington, DC, USA, 2022.
- (10) *Climate Change 2021: The Physical Science Basis. Contribution of Working Group I to the Sixth Assessment Report of the Intergovernmental Panel on Climate Change*; Masson-Delmotte, V., Zhai, P., Pirani, A., Connors, S. L., Péan, C., Berger, S., Caud, N., Chen, Y., Goldfarb, L., Gomis, M. I., Huang, M., Leitzell, K., Lonnoy, E., Matthews, J. B. R., Maycock, T. K., Waterfield, T., Yelekçi, O., Yu, R., Zhou, B., Eds.; Cambridge University Press: New York, NY, USA, 2021.
- (11) Franklin, J. The Atmospheric Degradation and Impact of 1,1,1,2-Tetrafluoroethane (Hydrofluorocarbon 134a). *Chemosphere* **1993**, *27*, 1565-1601.
- (12) U. S. Environmental Protection Agency. Significant New Alternatives Policy (SNAP) Regulations, <https://www.epa.gov/snap/snap-regulations> (accessed July 8, 2022).

- (13) Lee, Y.; Jung, D. A Brief Performance Comparison of R1234yf and R134a in a Bench Tester for Automobile Applications. *Appl. Therm. Eng.* **2012**, *35*, 240-242.
- (14) Navarro-Esbri, J.; Mendoza-Miranda, J. M.; Mota-Babiloni, A.; Barragán-Cervera, A.; Belman-Flores, J. M. Experimental Analysis of R1234yf as a Drop-In Replacement for R134a in a Vapor Compression System. *Int. J. Refrig.* **2013**, *36*, 870-880.
- (15) Mota-Babiloni, A.; Navarro-Esbri, J.; Barragán, Á.; Molés, F.; Peris, B. Drop-In Energy Performance Evaluation of R1234yf and R1234ze(E) in a Vapor Compression System as R134a Replacements. *Appl. Therm. Eng.* **2014**, *71*, 259-265.
- (16) Koyama, S.; Takata, N.; Fukuda, S. Drop-In Experiments on Heat Pump Cycle Using HFO-1234ze(E) and Its Mixtures with HFC-32. *13th International Refrigeration and Air Conditioning Conference*; West Lafayette, IN, USA, July 12-15, 2010.
- (17) Solstice® ze Refrigerant (HFO-1234ze (E)): The Environmental Alternative to Traditional Refrigerants; Honeywell Refrigerants: Heverlee, Belgium, 2018.
- (18) *ANSI/ASHRAE Standard 34-2019 Designation and Safety Classification of Refrigerants*; American Society of Heating, Refrigeration and Air-Conditioning Engineers: Atlanta, GA, USA, 2019.
- (19) Domanski, P. A.; McLinden, M. O.; Babushok, V. I.; Bell, I. H.; Fortin, T. J.; Hegetschweiler, M. J.; Huber, M. L.; Kedzierski, M. A.; Kim, D. K.; Lin, L.; Linteris, G. T.; Outcalt, S. L.; Payne, W. V.; Perkins, R. A.; Rowane, A.; Skye, H. *Low-GWP Non-Flammable Alternative Refrigerant Blends for HFC-134a: Final Report*; NISTIR 8455; National Institute for Standards and Technology: Gaithersburg, MD, USA, 2023.
- (20) Outcalt, S. L.; Rowane, A. J. Bubble Point Measurements of Mixtures of HFO and HFC Refrigerants. *J. Chem. Eng. Data* **2021**, *66*, 4670-4683.
- (21) Rowane, A. J.; Perkins, R. A. Speed of Sound Measurements of Binary Mixtures of 1,1,1,2-Tetrafluoroethane (R-134a), 2,3,3,3-Tetrafluoropropene (R-1234yf), and *trans*-1,3,3,3-Tetrafluoropropene (R-1234ze(E)) Refrigerants. *J. Chem. Eng. Data* **2022**, *67*, 1365-1377.
- (22) Bell, I. H. Mixture Models for Refrigerants R-1234yf/134a, R-1234yf/1234ze(E), and R-134a/1234ze(E) and Interim Models for R-125/1234yf, R-1234ze(E)/227ea, and R-1234yf/152a. *J. Phys. Chem. Ref. Data* **2022**, *51*, 013103.
- (23) Bell, I. H.; Riccardi, D.; Bazyleva, A.; McLinden, M. O. Survey of Data and Models for Refrigerant Mixtures Containing Halogenated Olefins. *J. Chem. Eng. Data* **2021**, *66*, 2335-2354.
- (24) Lemmon, E. W.; Bell, I. H.; Huber, M. L.; McLinden, M. O. *NIST Standard Reference Database 23: Reference Fluid Thermodynamic and Transport Properties (REFPROP)*, 10.0; National Institute of Standards and Technology: Gaithersburg, MD, USA, 2018.

- (25) Harris, G. L.; Torres, J. A. *Selected Laboratory and Measurement Practices and Procedures to Support Basic Mass Calibrations*; NISTIR 6969; National Institute of Standards and Technology: Gaithersburg, MD, USA, 2003.
- (26) Richter, M.; McLinden, M. O. Vapor-Phase ( $p, \rho, T, x$ ) Behavior and Virial Coefficients for the (Methane + Propane) System. *J. Chem. Eng. Data* **2014**, *59*, 4151-4164.
- (27) Kleinrahm, R.; Wagner, W. Measurement and Correlation of the Equilibrium Liquid and Vapour Densities and the Vapour Pressure Along the Coexistence Curve of Methane. *J. Chem. Thermodyn.* **1986**, *18*, 739-760.
- (28) Wagner, W.; Kleinrahm, R. Densimeters for Very Accurate Density Measurements of Fluids Over Large Ranges of Temperature, Pressure, and Density. *Metrologia* **2004**, *41*, S24-S39.
- (29) McLinden, M. O.; Lösch-Will, C. Apparatus for Wide-Ranging, High-Accuracy Fluid ( $p$ - $\rho$ - $T$ ) Measurements Based on a Compact Two-Sinker Densimeter. *J. Chem. Thermodyn.* **2007**, *39*, 507-530.
- (30) McLinden, M. O.; Kleinrahm, R.; Wagner, W. Force Transmission Errors in Magnetic Suspension Densimeters. *Int. J. Thermophys.* **2007**, *28*, 429-448.
- (31) Kleinrahm, R.; Yang, X.; McLinden, M. O.; Richter, M. Analysis of the Systemic Force-Transmission Error of the Magnetic-Suspension Coupling in Single-Sinker Densimeters and Commercial Gravimetric Sorption Analyzers. *Adsorption* **2019**, *25*, 717-735.
- (32) Richter, M.; McLinden, M. O.; Lemmon, E. W. Thermodynamic Properties of 2,3,3,3-Tetrafluoroprop-1-ene (R1234yf): Vapor Pressure and  $p$ - $\rho$ - $T$  Measurements and an Equation of State. *J. Chem. Eng. Data* **2011**, *56*, 3254-3264.
- (33) McLinden, M. O.; Splett, J. D. A Liquid Density Standard Over Wide Ranges of Temperature and Pressure Based on Toluene. *J. Res. Natl. Inst. Stand. Technol.* **2008**, *113*, 29-67.
- (34) McLinden, M. O. Thermodynamic Properties of Propane. I.  $p$ - $\rho$ - $T$  Behavior from (265 to 500) K with Pressures to 36 MPa. *J. Chem. Eng. Data* **2009**, *54*, 3181-3191.
- (35) Tillner-Roth, R.; Baehr, H. D. An International Standard Formulation for the Thermodynamic Properties of 1,1,1,2-Tetrafluoroethane (HFC-134a) for Temperatures from 170 K to 455 K and Pressures up to 70 MPa. *J. Phys. Chem. Ref. Data* **1994**, *23*, 657-729.
- (36) Thol, M.; Lemmon, E. W. Equation of State for the Thermodynamic Properties of *trans*-1,3,3,3-Tetrafluoropropene [R-1234ze(E)]. *Int. J. Thermophys.* **2016**, *37*, 28.
- (37) Yotsumoto, Y.; Sugitani, R.; Matsuo, S.; Sotani, T. Density Measurements of Binary Mixtures for (HFO-1234yf + HFC-134a) System. *31st Japan Symposium on Thermophysical Properties*; Fukuoka, Japan, November 17-19, 2010.

- (38) Al Ghafri, S. Z. S.; Rowland, D.; Akhfash, M.; Arami-Niya, A.; Khamphasith, M.; Xiao, X.; Tsuji, T.; Tanaka, Y.; Seiki, Y.; May, E. F.; Hughes, T. J. Thermodynamic Properties of Hydrofluoroolefin (R1234yf and R1234ze(E)) Refrigerant Mixtures: Density, Vapour-Liquid Equilibrium, and Heat Capacity Data and Modelling. *Int. J. Refrig.* **2019**, *98*, 249-260.
- (39) Zhang, H.; Dong, X.; Zhong, Q.; Li, H.; Gong, M.; Shen, J.; Wu, J. Investigation of  $p\rho T_x$  Properties for R1234ze(E) + R134a Mixtures in the Gas Phase. *Int. J. Refrig.* **2017**, *73*, 144-153.
- (40) Lemmon, E. W.; Akasaka, R. An International Standard Formulation for 2,3,3,3-Tetrafluoroprop-1-ene (R1234yf) Covering Temperatures from the Triple Point Temperature to 410 K and Pressures up to 100 MPa. *Int. J. Thermophys.* **2022**, *43*, 119.
- (41) Chen, Q.; Qi, H.; Zhang, S.; Hong, R.; Chen, G. An Experimental Study of  $PVT_x$  properties in the Gas Phase for Binary Mixtures of HFO-1234yf and HFC-134a. *Fluid Phase Equilib.* **2015**, *385*, 25-28.
- (42) Higashi, Y. Measurements of Thermodynamic Properties for the 50 Mass% R1234yf + 50 Mass% R1234ze(E) Blend. *Sci. Technol. Built Environ.* **2016**, *22*, 1185-1190.
- (43) Yang, J.; Fang, D.; Meng, X. Y.; Wu, J. T. Experimental Measurements and Correlations of the Vapor Phase  $p\nu T_x$  Behavior of Binary Mixtures of 1,1,1,2-Tetrafluoroethane (R134a)+2,3,3,3-Tetrafluoroprop-1-ene (R1234yf). *Int. J. Refrig.* **2021**, *132*, 263-275.
- (44) Hanwell, M. D.; Curtis, D. E.; Lonie, D. C.; Vandermeersch, T.; Zurek, E.; Hutchison, G. R. Avogadro: An Advanced Semantic Chemical Editor, Visualization, and Analysis Platform. *J. Cheminform.* **2012**, *4*, 17.

**Table 1. Chemical Information**

<b>Refrigerant</b>	<b>Chemical Name</b>	<b>Chemical Formula</b>	<b>CAS</b>	<b>Supplier<sup>a</sup></b>	<b>Purity<sup>b</sup></b>
R-134a	1,1,1,2-tetrafluoroethane	C <sub>2</sub> H <sub>2</sub> F <sub>4</sub>	811-97-2	Dupont	0.999
R-1234yf	2,3,3,3-tetrafluoropropene	C <sub>3</sub> H <sub>2</sub> F <sub>4</sub>	754-12-1	Chemours	0.999
R-1234ze(E)	<i>trans</i> -1,3,3,3-tetrafluoropropene	C <sub>3</sub> H <sub>2</sub> F <sub>4</sub>	29118-24-9	Honeywell	0.9997

<sup>a</sup>In order to describe materials and experimental procedures adequately, it is occasionally necessary to identify commercial products by manufacturers' names or labels. In no instance does such identification imply endorsement by the National Institute of Standards and Technology, nor does it imply that the particular product or equipment is necessarily the best available for the purpose. <sup>b</sup>Supplier's stated purity in mole fraction.

**Table 2. Measured Refrigerant Blends**

<b>Blend</b>	$x_1^a$	$x_2^a$	<b>Sample Volume</b>
R-1234yf + R-134a	0.33634	0.66366	10 L
	0.64709	0.35291	10 L
R-134a + R-1234ze(E)	0.33250	0.66750	13.4 L
	0.66356	0.33644	13.4 L
R-1234yf + R-1234ze(E)	0.33584	0.66416	13.4 L
	0.66660	0.33340	13.4 L

<sup>a</sup>Molar composition of first (1) and second (2) component. Standard uncertainty in molar composition from gravimetric preparation estimated at 0.00005.

**Table 3. Measured Temperature ( $T$ ), Pressure ( $p$ ), and Density ( $\rho$ ) Data for the 0.33634/0.66366 Molar R-1234yf + R-134a Blend<sup>a</sup>**

$T^b$ /K	$p$ /MPa	$\rho$ /kg·m <sup>-3</sup>	$u(p)^c$ /kPa	$100 \cdot (U(\rho)/\rho)^d$	$\Delta\rho^e$
<b>Vapor-phase</b>					
293.154	0.0645	2.847	0.030	0.140	0.013
293.156	0.1202	5.369	0.030	0.086	0.001
293.156	0.1813	8.215	0.030	0.066	-0.002
293.156	0.2435	11.203	0.030	0.054	-0.005
293.156	0.3038	14.196	0.030	0.050	-0.009
293.154	0.3601	17.079	0.030	0.048	-0.013
293.157	0.4207	20.292	0.030	0.047	-0.017
283.158	0.0616	2.819	0.030	0.154	0.011
283.158	0.1024	4.733	0.030	0.092	0.001
283.156	0.1513	7.084	0.030	0.068	-0.002
283.155	0.1844	8.710	0.030	0.061	-0.007
283.156	0.2242	10.712	0.030	0.056	-0.008
283.159	0.2682	12.975	0.030	0.054	-0.011
283.159	0.3068	15.018	0.030	0.051	-0.015
283.158	0.3406	16.850	0.030	0.048	-0.021
283.157	0.3810	19.100	0.030	0.047	-0.028
273.156	0.0591	2.806	0.030	0.146	-0.005
273.157	0.0854	4.087	0.030	0.104	-0.009
273.158	0.1103	5.314	0.030	0.087	-0.007
273.157	0.1557	7.609	0.030	0.066	-0.009
273.156	0.1557	7.609	0.030	0.067	-0.010
273.157	0.1864	9.198	0.030	0.065	-0.012
273.158	0.2055	10.205	0.030	0.057	-0.014
273.158	0.2323	11.640	0.030	0.054	-0.019
273.156	0.2569	12.982	0.030	0.053	-0.024
263.157	0.0460	2.260	0.030	0.195	-0.024
263.158	0.0604	2.986	0.030	0.136	-0.021
263.157	0.0803	3.993	0.030	0.107	-0.016
263.160	0.1010	5.060	0.030	0.089	-0.012
263.157	0.1207	6.089	0.030	0.080	-0.015
263.159	0.1410	7.166	0.030	0.071	-0.015
263.159	0.1603	8.206	0.030	0.068	-0.019
263.157	0.1800	9.285	0.030	0.061	-0.022
253.155	0.0439	2.247	0.030	0.185	-0.030
253.157	0.0615	3.169	0.030	0.141	-0.024
253.156	0.0764	3.964	0.030	0.108	-0.022
253.155	0.0908	4.738	0.030	0.094	-0.023
253.157	0.1064	5.585	0.030	0.090	-0.024
253.157	0.1214	6.410	0.030	0.112	-0.046
253.158	0.1310	6.949	0.030	0.075	-0.028
<b>Liquid-phase and supercritical states</b>					
230.018	1.0580	1377.826	1.310	0.044	-0.088
240.013	4.0963	1357.442	1.880	0.045	-0.082
240.015	2.5159	1353.415	1.770	0.045	-0.080

240.017	1.4524	1350.630	2.110	0.046	-0.079
249.999	10.5100	1346.407	1.720	0.044	-0.082
250.005	8.7759	1341.986	1.630	0.044	-0.081
250.005	7.1240	1337.663	1.670	0.044	-0.079
250.007	5.5510	1333.409	1.340	0.043	-0.077
250.008	4.0545	1329.242	1.480	0.044	-0.074
250.007	1.5145	1321.869	1.600	0.044	-0.070
260.006	9.9758	1318.072	1.880	0.045	-0.073
260.007	9.9633	1318.033	1.310	0.043	-0.073
260.009	8.4082	1313.584	1.720	0.044	-0.071
260.006	5.5224	1304.933	1.650	0.044	-0.067
260.008	4.1799	1300.704	1.540	0.044	-0.065
260.007	1.6898	1292.499	1.400	0.043	-0.060
269.996	9.5071	1288.959	1.360	0.043	-0.066
269.999	8.1308	1284.487	1.300	0.043	-0.065
269.998	5.5607	1275.751	1.470	0.044	-0.060
270.000	4.3642	1271.460	1.240	0.043	-0.059
269.999	2.1263	1263.066	1.520	0.044	-0.053
280.001	9.3448	1259.774	1.450	0.043	-0.058
280.002	8.1207	1255.273	1.530	0.044	-0.056
280.004	6.9506	1250.820	1.560	0.044	-0.054
280.002	4.7599	1242.075	1.530	0.044	-0.050
280.002	3.7350	1237.760	1.380	0.043	-0.048
280.002	1.8257	1229.313	1.400	0.043	-0.042
295.002	11.6644	1224.821	1.700	0.044	-0.048
295.004	9.4728	1215.562	1.440	0.043	-0.044
295.002	7.4650	1206.491	1.390	0.043	-0.040
295.005	5.6268	1197.557	1.450	0.043	-0.035
295.003	3.9359	1188.754	1.270	0.043	-0.029
295.006	2.3907	1180.086	1.230	0.043	-0.023
309.994	10.9365	1175.985	1.560	0.044	-0.030
309.995	10.0284	1171.275	1.390	0.043	-0.028
309.994	8.3389	1162.045	1.430	0.043	-0.023
309.994	6.0525	1148.363	1.380	0.043	-0.014
309.994	4.0426	1134.895	1.320	0.043	-0.003
309.994	3.4281	1130.445	1.180	0.043	0.001
325.000	10.8845	1126.955	1.300	0.043	-0.009
325.003	8.7591	1112.711	1.350	0.043	0.001
325.000	6.3020	1093.916	1.220	0.043	0.018
325.000	4.2424	1075.417	1.350	0.043	0.037
325.002	2.5330	1057.237	1.170	0.043	0.057
339.995	8.5376	1054.188	1.260	0.043	0.040
339.995	6.7029	1035.338	1.250	0.043	0.063
339.996	5.1481	1016.460	1.150	0.043	0.089
339.998	4.1586	1002.423	1.100	0.043	0.110
339.995	2.5735	974.715	1.190	0.043	0.152
344.995	4.1228	973.808	1.120	0.043	0.150
349.993	5.6824	972.934	1.130	0.043	0.139
354.997	7.2509	972.074	1.120	0.043	0.126
359.997	8.8220	971.227	1.160	0.043	0.110

359.997	7.5860	952.038	1.090	0.043	0.146
359.998	6.1086	923.684	1.110	0.043	0.209
360.000	4.8368	890.823	1.110	0.043	0.297
359.998	3.5803	839.398	1.060	0.043	-1.991
364.997	4.5969	838.738	1.050	0.043	-1.654
369.997	5.6303	838.099	1.050	0.043	-1.397
375.000	6.6756	837.454	1.080	0.043	-1.193
379.995	7.7285	836.813	1.060	0.043	-1.011
379.996	6.8787	805.894	1.100	0.043	-1.089
379.996	6.2346	774.668	1.050	0.043	-1.114
379.997	5.1658	681.602	1.060	0.043	-1.031
384.996	5.8201	681.232	1.050	0.043	-0.935
389.995	6.4842	680.856	1.050	0.043	-0.846
394.995	7.1546	680.451	1.060	0.043	-0.776
400.001	7.8310	680.028	1.050	0.043	-0.712
400.000	7.0689	616.989	1.070	0.043	-0.650
399.998	5.9662	460.147	1.070	0.043	-0.451
400.000	5.0344	305.066	1.090	0.049	0.578
400.000	3.8495	183.201	1.110	0.058	0.161
400.000	2.9176	121.603	1.120	0.073	0.030
400.003	1.7421	63.903	1.140	0.128	-0.132

<sup>a</sup>Reported values are averages of replicate measurements at each  $(T, p)$  state point. <sup>b</sup>Standard uncertainty in temperature is 3 mK. <sup>c</sup>Standard uncertainty in pressure. <sup>d</sup>Relative combined, expanded ( $k = 2$ ) state-point uncertainty in density. <sup>e</sup>Relative deviation from default equation of state calculated according to eq 3.

**Table 4. Measured Temperature ( $T$ ), Pressure ( $p$ ), and Density ( $\rho$ ) Data for the 0.64709/0.35291 Molar R-1234yf + R-134a Blend<sup>a</sup>**

$T^b$ /K	$p$ /MPa	$\rho$ /kg·m <sup>-3</sup>	$u(p)^c$ /kPa	$100 \cdot (U(\rho)/\rho)^d$	$\Delta\rho^e$
<b>Vapor-phase</b>					
293.156	0.0660	3.024	0.030	0.130	0.185
293.155	0.1241	5.762	0.030	0.083	0.205
293.154	0.1874	8.833	0.030	0.061	0.212
293.155	0.2418	11.555	0.030	0.054	0.215
293.157	0.3059	14.865	0.030	0.050	0.217
293.155	0.3654	18.045	0.030	0.048	0.216
293.155	0.4237	21.280	0.030	0.046	0.213
293.155	0.4801	24.530	0.030	0.046	0.209
283.154	0.0625	2.968	0.030	0.137	0.201
283.155	0.1042	4.999	0.030	0.089	0.211
283.156	0.1422	6.894	0.030	0.071	0.214
283.158	0.1879	9.226	0.030	0.060	0.215
283.157	0.2286	11.356	0.030	0.055	0.215
283.157	0.2648	13.299	0.030	0.052	0.213
283.156	0.3048	15.499	0.030	0.050	0.211
283.155	0.3462	17.841	0.030	0.048	0.206
283.155	0.3815	19.892	0.030	0.047	0.202
273.153	0.0674	3.327	0.030	0.126	0.191
273.152	0.0932	4.638	0.030	0.095	0.198
273.153	0.1291	6.498	0.030	0.074	0.202
273.152	0.1513	7.670	0.030	0.067	0.203
273.151	0.1823	9.331	0.030	0.060	0.203
273.152	0.2106	10.885	0.030	0.056	0.201
273.151	0.2449	12.804	0.030	0.053	0.197
273.151	0.2755	14.567	0.030	0.051	0.192
263.156	0.0442	2.252	0.030	0.182	0.169
263.156	0.0696	3.581	0.030	0.119	0.184
263.156	0.0818	4.224	0.030	0.103	0.189
263.156	0.1050	5.469	0.030	0.084	0.193
263.155	0.1269	6.663	0.030	0.074	0.194
263.155	0.1476	7.807	0.030	0.067	0.192
263.156	0.1671	8.903	0.030	0.063	0.191
263.154	0.1854	9.953	0.030	0.059	0.188
253.154	0.0413	2.189	0.030	0.191	0.154
253.154	0.0569	3.040	0.030	0.140	0.166
253.155	0.0718	3.859	0.030	0.113	0.174
253.153	0.0861	4.650	0.030	0.096	0.176
253.154	0.1014	5.514	0.030	0.085	0.179
253.154	0.1161	6.352	0.030	0.077	0.178
253.153	0.1302	7.164	0.030	0.071	0.174
<b>Liquid-phase and supercritical states</b>					
230.002	0.9129	1336.222	2.220	0.046	-0.250
239.998	1.0656	1309.005	1.410	0.044	-0.243
239.998	1.0654	1309.002	1.340	0.044	-0.243

249.997	5.6268	1294.296	1.880	0.045	-0.239
249.998	4.1646	1290.030	1.930	0.045	-0.238
249.998	1.6135	1282.248	1.700	0.044	-0.235
259.997	9.4760	1278.562	1.630	0.044	-0.232
259.999	7.9771	1274.037	1.500	0.044	-0.232
259.997	5.2636	1265.460	1.300	0.043	-0.230
260.000	3.9997	1261.256	1.280	0.043	-0.228
259.999	1.6695	1253.139	1.430	0.044	-0.226
269.994	8.9007	1249.632	1.880	0.045	-0.221
269.997	7.5848	1245.110	1.420	0.043	-0.221
269.997	6.3404	1240.695	1.540	0.044	-0.220
269.998	4.0551	1232.170	1.490	0.044	-0.218
269.998	1.9837	1223.903	1.440	0.044	-0.215
280.001	8.6324	1220.574	1.520	0.044	-0.208
280.001	7.4701	1216.029	1.430	0.043	-0.207
280.001	5.3397	1207.255	1.400	0.043	-0.205
280.003	3.4025	1198.696	1.270	0.043	-0.204
280.003	1.6538	1190.428	1.490	0.044	-0.201
295.003	10.5574	1185.253	1.400	0.043	-0.184
295.004	9.5151	1180.602	1.420	0.043	-0.183
295.003	7.5911	1171.564	1.330	0.043	-0.181
295.006	5.8285	1162.653	1.370	0.043	-0.179
295.003	4.2090	1153.865	1.550	0.044	-0.176
295.003	2.0565	1141.048	1.290	0.043	-0.173
309.994	9.9070	1137.041	1.290	0.043	-0.150
309.999	8.2738	1127.710	1.360	0.043	-0.147
309.996	6.0975	1114.100	1.390	0.043	-0.142
309.997	4.1900	1100.709	1.350	0.043	-0.137
309.995	2.0300	1083.314	1.550	0.044	-0.133
325.002	8.6631	1079.822	1.250	0.043	-0.105
325.003	8.0389	1075.113	1.260	0.043	-0.103
325.001	5.8321	1056.789	1.300	0.043	-0.093
325.002	3.9882	1038.780	1.290	0.043	-0.085
325.002	2.1197	1016.674	1.290	0.043	-0.082
339.997	7.5365	1013.684	1.220	0.043	-0.045
339.997	5.9388	995.132	1.110	0.043	-0.030
339.997	4.0329	967.739	1.170	0.043	-0.005
339.996	2.6132	940.709	1.120	0.043	0.018
344.995	4.0306	939.822	1.080	0.043	0.040
349.994	5.4566	938.944	1.130	0.043	0.047
354.994	6.8882	938.074	1.110	0.043	0.045
359.998	8.3245	937.211	1.130	0.043	0.036
359.998	6.4863	904.331	1.140	0.043	0.099
359.998	5.0077	867.438	1.070	0.043	-1.083
359.999	3.5874	807.729	1.050	0.043	-1.653
364.998	4.5147	807.094	1.040	0.043	-1.370
369.998	5.4569	806.465	1.050	0.043	-1.150
374.998	6.4088	805.824	1.060	0.043	-0.973
379.998	7.3671	805.163	1.060	0.043	-0.821
379.997	6.5403	772.197	1.080	0.043	-0.980

379.998	5.5548	711.582	1.050	0.043	-1.130
384.998	5.2431	595.069	1.050	0.043	-1.043
389.997	5.7521	594.706	1.050	0.043	-0.982
394.997	6.2654	594.329	1.050	0.043	-0.936
399.999	6.7829	593.964	1.050	0.043	-0.893
400.002	5.8985	475.041	1.060	0.043	-0.760
400.001	4.9850	322.447	1.080	0.048	1.321
400.001	3.9471	203.238	1.100	0.056	0.831
400.001	2.7047	115.490	1.110	0.078	0.461
400.003	1.7401	66.680	1.120	0.120	0.196

---

<sup>a</sup>Reported values are averages of replicate measurements at each  $(T, p)$  state point. <sup>b</sup>Standard uncertainty in temperature is 3 mK. <sup>c</sup>Standard uncertainty in pressure. <sup>d</sup>Relative combined, expanded ( $k = 2$ ) state-point uncertainty in density. <sup>e</sup>Relative deviation from default equation of state calculated according to eq 3.

**Table 5. Measured Temperature ( $T$ ), Pressure ( $p$ ), and Density ( $\rho$ ) Data for the 0.33250/0.66750 Molar R-134a + R-1234ze(E) Blend<sup>a</sup>**

$T^b$ /K	$p$ /MPa	$\rho$ /kg·m <sup>-3</sup>	$u(p)^c$ /kPa	$100 \cdot (U(\rho)/\rho)^d$	$\Delta\rho^e$
<b>Vapor-phase</b>					
293.156	0.0577	2.640	0.030	0.170	-0.012
293.156	0.0577	2.640	0.030	0.147	-0.012
293.157	0.1025	4.739	0.030	0.097	-0.022
293.159	0.1415	6.606	0.030	0.071	-0.030
293.159	0.1818	8.574	0.030	0.062	-0.041
293.157	0.2212	10.545	0.030	0.056	-0.050
293.158	0.2624	12.649	0.030	0.053	-0.060
293.157	0.3013	14.681	0.030	0.050	-0.071
293.157	0.3417	16.848	0.030	0.049	-0.080
293.159	0.3807	18.993	0.030	0.047	-0.090
283.155	0.0603	2.864	0.030	0.140	-0.010
283.156	0.0947	4.540	0.030	0.094	-0.019
283.157	0.1255	6.070	0.030	0.076	-0.024
283.155	0.1532	7.466	0.030	0.067	-0.030
283.155	0.1838	9.042	0.030	0.060	-0.036
283.157	0.2107	10.449	0.030	0.057	-0.042
283.158	0.2430	12.172	0.030	0.053	-0.048
283.157	0.2701	13.645	0.030	0.051	-0.053
283.156	0.3015	15.394	0.030	0.050	-0.060
273.158	0.0496	2.438	0.030	0.166	-0.037
273.155	0.0751	3.720	0.030	0.119	-0.029
273.155	0.1059	5.298	0.030	0.085	-0.027
273.154	0.1269	6.393	0.030	0.074	-0.028
273.155	0.1524	7.744	0.030	0.071	-0.029
273.155	0.1754	8.986	0.030	0.061	-0.030
273.158	0.2011	10.397	0.030	0.057	-0.033
263.161	0.0377	1.917	0.030	0.246	-0.051
263.161	0.0628	3.225	0.030	0.133	-0.033
263.158	0.0860	4.454	0.030	0.098	-0.023
263.156	0.1004	5.231	0.030	0.094	-0.020
263.156	0.1206	6.333	0.030	0.076	-0.019
263.158	0.1452	7.697	0.030	0.067	-0.015
263.160	0.1565	8.337	0.030	0.069	-0.013
253.167	0.0361	1.913	0.030	0.215	-0.053
253.163	0.0455	2.419	0.030	0.171	-0.041
253.163	0.0606	3.244	0.030	0.136	-0.025
253.163	0.0760	4.094	0.030	0.113	-0.019
253.164	0.0905	4.906	0.030	0.093	-0.012
<b>Liquid-phase and supercritical states</b>					
230.011	0.9394	1379.400	2.000	0.046	0.063
230.011	0.9406	1379.399	1.980	0.045	0.063
230.010	0.9415	1379.406	1.510	0.044	0.063
245.008	14.0797	1368.702	1.800	0.044	0.059
245.008	14.0809	1368.706	1.760	0.044	0.059

245.013	11.8529	1364.114	1.630	0.044	0.067
245.011	7.7628	1355.309	1.910	0.045	0.080
245.012	4.0497	1346.804	1.780	0.045	0.093
245.015	1.3037	1340.152	1.630	0.044	0.104
259.998	15.4282	1335.162	1.960	0.045	0.084
260.001	13.4513	1330.555	1.460	0.044	0.090
260.000	11.5561	1326.008	1.680	0.044	0.096
260.000	8.0154	1317.091	1.350	0.043	0.109
260.001	3.2733	1304.149	1.750	0.044	0.126
260.002	1.8343	1299.957	1.250	0.043	0.132
279.999	18.6287	1294.065	1.580	0.044	0.100
280.001	15.1497	1284.618	1.560	0.044	0.110
280.002	11.9529	1275.346	1.400	0.043	0.121
280.002	7.6359	1261.735	1.470	0.043	0.136
280.002	3.8416	1248.486	1.550	0.044	0.152
280.004	1.5806	1239.867	1.480	0.043	0.163
304.997	19.1997	1233.418	1.480	0.043	0.117
304.998	16.3851	1223.766	1.640	0.044	0.125
304.998	12.5769	1209.525	1.390	0.043	0.137
304.997	8.1739	1190.905	1.500	0.043	0.153
304.997	4.4490	1172.669	1.630	0.044	0.171
304.997	1.3205	1154.826	1.480	0.043	0.190
309.996	4.0729	1153.572	1.410	0.043	0.178
319.988	9.5779	1151.337	1.380	0.043	0.158
329.988	15.0584	1149.270	1.260	0.043	0.143
339.994	20.5176	1147.396	1.500	0.043	0.132
339.994	15.6050	1122.887	1.480	0.043	0.148
339.994	12.3122	1103.559	1.400	0.043	0.164
339.994	8.2775	1074.984	1.430	0.043	0.191
339.997	4.2837	1037.485	1.120	0.043	0.239
339.994	2.4419	1014.333	1.200	0.043	0.274
349.993	6.0373	1012.627	1.140	0.043	0.245
359.995	9.6560	1011.043	1.100	0.043	0.211
369.995	13.2785	1009.528	1.130	0.043	0.182
379.994	16.8941	1008.053	1.160	0.043	0.163
379.994	13.7847	978.471	1.200	0.043	0.182
379.994	10.9640	944.282	1.170	0.043	0.213
379.996	8.1077	895.878	1.090	0.043	0.275
379.996	5.0540	795.138	1.080	0.044	0.477
384.994	5.9659	794.625	1.050	0.043	0.399
389.994	6.8887	794.099	1.050	0.044	0.334
394.993	7.8192	793.564	1.060	0.044	0.285
399.997	8.7564	793.013	1.060	0.044	0.249
399.998	7.2824	727.654	1.070	0.044	-0.465
399.998	6.1375	629.407	1.060	0.044	-0.151
399.998	5.0688	399.698	1.080	0.044	0.264
399.998	3.8717	206.293	1.110	0.056	-0.758
399.998	2.5929	110.897	1.120	0.080	-0.418

---

<sup>a</sup>Reported values are averages of replicate measurements at each  $(T, p)$  state point. <sup>b</sup>Standard uncertainty in temperature is 3 mK. <sup>c</sup>Standard uncertainty in pressure. <sup>d</sup>Relative combined, expanded ( $k = 2$ ) state-point uncertainty in density. <sup>e</sup>Relative deviation from default equation of state calculated according to eq 3.

**Table 6. Measured Temperature ( $T$ ), Pressure ( $p$ ), and Density ( $\rho$ ) Data for the 0.66356/0.33644 Molar R-134a + R-1234ze(E) Blend<sup>a</sup>**

$T^b$ /K	$p$ /MPa	$\rho$ /kg·m <sup>-3</sup>	$u(p)^c$ /kPa	$100 \cdot (U(\rho)/\rho)^d$	$\Delta\rho^e$
<b>Vapor-phase</b>					
293.154	0.0537	2.364	0.030	0.160	-0.039
293.157	0.1002	4.458	0.030	0.093	-0.040
293.158	0.1512	6.808	0.030	0.072	-0.048
293.160	0.2037	9.290	0.030	0.059	-0.059
293.159	0.2550	11.783	0.030	0.053	-0.072
293.159	0.3029	14.175	0.030	0.051	-0.086
293.158	0.3501	16.597	0.030	0.048	-0.100
293.157	0.4017	19.330	0.030	0.047	-0.119
293.159	0.4504	21.986	0.030	0.046	-0.139
283.154	0.0511	2.329	0.030	0.183	-0.043
283.155	0.1060	4.903	0.030	0.089	-0.043
283.157	0.1536	7.203	0.030	0.068	-0.050
283.157	0.2028	9.644	0.030	0.058	-0.060
283.158	0.2510	12.108	0.030	0.053	-0.073
283.158	0.3013	14.762	0.030	0.050	-0.089
273.158	0.0489	2.313	0.030	0.176	-0.055
273.156	0.0815	3.895	0.030	0.110	-0.044
273.156	0.1208	5.844	0.030	0.080	-0.045
273.155	0.1640	8.046	0.030	0.064	-0.051
273.157	0.2017	10.021	0.030	0.063	-0.060
263.158	0.0468	2.302	0.030	0.176	-0.059
263.157	0.0780	3.880	0.030	0.114	-0.044
263.156	0.1066	5.359	0.030	0.085	-0.042
263.154	0.1329	6.745	0.030	0.072	-0.046
263.154	0.1571	8.047	0.030	0.069	-0.051
253.162	0.0449	2.301	0.030	0.212	-0.074
253.159	0.0651	3.361	0.030	0.138	-0.049
253.158	0.0933	4.875	0.030	0.101	-0.043
253.155	0.1108	5.835	0.030	0.088	-0.042
<b>Liquid-phase and supercritical states</b>					
230.010	0.9660	1402.623	4.520	0.055	0.096
230.008	0.9664	1402.628	5.550	0.061	0.096
230.009	0.9685	1402.626	4.140	0.054	0.096
245.011	12.0545	1386.704	1.590	0.044	0.095
245.011	12.0501	1386.694	1.780	0.044	0.094
245.015	9.9507	1382.143	1.490	0.044	0.101
245.013	7.9658	1377.720	1.510	0.044	0.108
245.012	4.2867	1369.139	1.610	0.044	0.121
245.015	1.4247	1362.070	1.840	0.044	0.133
260.002	15.7690	1356.808	1.700	0.044	0.109
260.003	14.0266	1352.679	1.400	0.043	0.114
260.005	12.1366	1348.071	1.710	0.044	0.120
260.003	8.6022	1339.042	1.840	0.044	0.132
260.004	3.8612	1325.928	1.660	0.044	0.151

260.007	1.3602	1318.456	1.170	0.043	0.163
280.000	18.3309	1312.269	1.910	0.044	0.122
280.001	14.9347	1302.734	1.580	0.044	0.132
280.003	11.8171	1293.387	1.540	0.043	0.142
280.002	7.6041	1279.684	1.550	0.044	0.159
280.003	3.8965	1266.338	1.450	0.043	0.178
280.008	1.6836	1257.638	1.280	0.043	0.192
304.999	19.5685	1250.996	1.420	0.043	0.130
304.999	15.4975	1236.448	1.530	0.043	0.143
304.999	11.8883	1222.160	1.320	0.043	0.157
304.999	7.7058	1203.446	1.400	0.043	0.179
304.999	4.1635	1185.110	1.320	0.043	0.205
304.999	1.8789	1171.601	1.170	0.043	0.228
314.993	7.4882	1169.120	1.190	0.043	0.189
339.999	21.4741	1164.055	1.370	0.043	0.129
339.996	15.6947	1134.447	1.480	0.043	0.152
339.996	11.8006	1110.170	1.280	0.043	0.179
339.998	8.0475	1081.430	1.190	0.043	0.221
339.998	3.9440	1038.951	1.150	0.043	0.306
339.997	2.3054	1015.610	1.160	0.043	0.366
349.993	5.8380	1013.890	1.090	0.043	0.300
359.998	9.4056	1012.324	1.090	0.043	0.243
369.995	12.9836	1010.853	1.170	0.043	0.197
379.996	16.5642	1009.426	1.140	0.043	0.163
379.997	14.1225	984.560	1.210	0.043	0.190
379.997	11.0710	945.135	1.110	0.043	0.244
379.998	7.9933	886.503	1.080	0.043	0.350
379.998	5.1089	765.284	1.060	0.044	0.630
384.995	5.9415	764.838	1.050	0.044	0.518
389.995	6.7866	764.396	1.050	0.044	0.431
394.995	7.6409	763.955	1.060	0.044	0.366
399.999	8.5026	763.500	1.060	0.044	0.318
399.998	6.0369	536.799	1.760	0.044	0.046
400.003	3.7067	175.446	1.110	0.059	-0.592
400.001	1.5025	54.037	1.140	0.142	-0.357

<sup>a</sup>Reported values are averages of replicate measurements at each  $(T, p)$  state point. <sup>b</sup>Standard uncertainty in temperature is 3 mK. <sup>c</sup>Standard uncertainty in pressure. <sup>d</sup>Relative combined, expanded ( $k = 2$ ) state-point uncertainty in density. <sup>e</sup>Relative deviation from default equation of state calculated according to eq 3.

**Table 7. Measured Temperature ( $T$ ), Pressure ( $p$ ), and Density ( $\rho$ ) Data for the 0.33584/0.66416 Molar R-1234yf + R-1234ze(E) Blend<sup>a</sup>**

$T^b$ /K	$p$ /MPa	$\rho$ /kg·m <sup>-3</sup>	$u(p)^c$ /kPa	$100 \cdot (U(\rho)/\rho)^d$	$\Delta\rho^e$
<b>Vapor-phase</b>					
293.153	0.1061	5.092	0.030	0.086	-0.009
293.154	0.1509	7.323	0.030	0.072	-0.004
293.158	0.2004	9.856	0.030	0.058	0.000
293.159	0.2535	12.651	0.030	0.054	0.005
293.158	0.3023	15.303	0.030	0.050	0.011
293.156	0.3517	18.067	0.030	0.048	0.019
293.156	0.3755	19.431	0.030	0.047	0.024
293.156	0.4052	21.172	0.030	0.046	0.032
293.158	0.4144	21.715	0.030	0.046	0.035
293.159	0.4193	22.010	0.030	0.046	0.037
283.150	0.0765	3.784	0.030	0.112	-0.012
283.150	0.1235	6.190	0.030	0.076	0.001
283.150	0.1635	8.289	0.030	0.064	0.007
283.150	0.2026	10.400	0.030	0.057	0.015
283.150	0.2436	12.667	0.030	0.053	0.025
283.150	0.2626	13.743	0.030	0.052	0.030
283.152	0.2826	14.887	0.030	0.051	0.037
283.153	0.3025	16.048	0.030	0.049	0.045
283.153	0.3172	16.913	0.030	0.049	0.052
273.157	0.0565	2.884	0.030	0.149	-0.055
273.156	0.0813	4.182	0.030	0.106	-0.029
273.156	0.1041	5.396	0.030	0.086	-0.011
273.158	0.1251	6.533	0.030	0.079	-0.001
273.157	0.1506	7.934	0.030	0.068	0.011
273.157	0.1789	9.520	0.030	0.060	0.023
273.158	0.2038	10.942	0.030	0.058	0.037
273.159	0.2259	12.228	0.030	0.054	0.049
263.155	0.0592	3.149	0.030	0.135	-0.026
263.153	0.0824	4.421	0.030	0.101	-0.008
263.154	0.1038	5.616	0.030	0.087	0.007
263.155	0.1236	6.739	0.030	0.074	0.023
263.156	0.1420	7.797	0.030	0.067	0.036
253.155	0.0395	2.173	0.030	0.196	-0.056
253.152	0.0631	3.506	0.030	0.126	-0.015
253.153	0.0849	4.760	0.030	0.099	0.012
253.153	0.1050	5.942	0.030	0.082	0.037
<b>Liquid-phase and supercritical states</b>					
230.007	0.8785	1338.848	1.240	0.044	0.166
230.004	0.8784	1338.855	1.250	0.044	0.166
240.002	6.0635	1325.128	2.100	0.046	0.174
240.004	4.2971	1321.034	1.400	0.044	0.181
240.008	2.6144	1317.007	1.460	0.044	0.187
240.003	1.2210	1313.598	1.480	0.044	0.193
240.001	1.2192	1313.601	1.610	0.044	0.193

250.000	10.2449	1310.027	1.480	0.044	0.183
250.002	8.6455	1306.194	1.480	0.044	0.188
250.001	5.2842	1297.786	2.080	0.045	0.201
250.001	2.2463	1289.697	1.780	0.045	0.214
250.001	1.2161	1286.830	1.750	0.045	0.218
259.997	9.4610	1283.176	1.740	0.044	0.207
259.999	7.8657	1278.858	1.380	0.043	0.213
259.999	6.3384	1274.596	1.540	0.044	0.219
259.997	3.4947	1266.270	1.650	0.044	0.231
259.999	1.2244	1259.202	1.740	0.044	0.242
269.995	8.9146	1255.977	1.660	0.044	0.229
269.996	7.4946	1251.634	1.290	0.043	0.235
269.999	6.1361	1247.333	1.480	0.044	0.241
269.995	3.5969	1238.910	1.520	0.044	0.253
269.998	1.3082	1230.781	1.450	0.044	0.265
280.000	8.3908	1227.760	1.350	0.043	0.252
280.003	7.1401	1223.389	1.350	0.043	0.258
280.002	4.7941	1214.791	1.480	0.044	0.270
280.004	2.6527	1206.367	1.240	0.043	0.281
280.004	1.6538	1202.235	1.430	0.043	0.288
295.003	11.4295	1198.217	1.320	0.043	0.271
295.003	9.1251	1189.218	1.320	0.043	0.282
295.005	6.0232	1175.988	1.240	0.043	0.299
295.006	4.1647	1167.315	1.200	0.043	0.311
295.005	1.6703	1154.569	1.250	0.043	0.329
310.001	10.1307	1150.870	1.280	0.043	0.315
310.003	8.2971	1141.824	1.120	0.043	0.327
310.002	5.8190	1128.431	1.210	0.043	0.346
310.005	4.3378	1119.616	1.200	0.043	0.359
310.000	1.7393	1102.274	1.250	0.043	0.384
314.997	4.1434	1101.096	1.160	0.043	0.381
319.994	6.5523	1100.014	1.100	0.043	0.378
324.992	8.9554	1098.971	1.160	0.043	0.374
324.993	6.8865	1085.356	1.130	0.043	0.396
324.994	5.0665	1071.889	1.170	0.043	0.420
324.994	3.4732	1058.570	1.170	0.043	0.445
324.995	1.6645	1041.020	1.090	0.043	0.478
329.991	3.6507	1040.015	1.120	0.043	0.477
334.990	5.6443	1039.089	1.140	0.043	0.471
339.997	7.6438	1038.201	1.150	0.043	0.462
339.998	6.1684	1024.498	1.100	0.043	0.494
339.999	4.8765	1010.886	1.110	0.043	0.528
340.000	3.4112	992.893	1.100	0.043	0.581
339.999	1.9414	970.612	1.150	0.043	0.657
349.995	5.1157	968.963	1.090	0.043	0.623
359.999	8.3224	967.480	1.080	0.043	0.570
360.000	7.2699	953.571	1.110	0.043	0.617
360.001	6.0693	935.147	1.080	0.043	0.690
360.002	5.0695	916.772	1.070	0.043	0.782
360.001	4.0668	893.912	1.080	0.043	0.931

370.001	6.5746	892.622	1.060	0.043	0.782
379.996	9.1113	891.418	1.070	0.043	0.666
379.997	7.5161	858.682	1.100	0.043	0.809
380.000	6.0721	816.851	1.070	0.043	1.082
379.998	5.0511	770.578	1.060	0.043	-3.774
380.000	4.0354	659.769	1.040	0.043	-2.851
384.996	4.6161	659.412	1.040	0.043	-2.590
389.997	5.2107	659.057	1.040	0.043	-2.361
394.994	5.8140	658.684	1.050	0.043	-2.167
400.001	6.4254	658.307	1.070	0.043	-2.006
400.001	5.4779	532.493	1.060	0.043	-1.383
400.002	4.1095	250.121	1.090	0.052	0.721
399.997	2.7673	127.701	1.110	0.074	0.083
400.005	1.6855	67.553	1.120	0.123	-0.159
400.002	0.9734	36.215	1.600	0.418	-0.326

<sup>a</sup>Reported values are averages of replicate measurements at each  $(T, p)$  state point. <sup>b</sup>Standard uncertainty in temperature is 3 mK. <sup>c</sup>Standard uncertainty in pressure. <sup>d</sup>Relative combined, expanded ( $k = 2$ ) state-point uncertainty in density. <sup>e</sup>Relative deviation from default equation of state calculated according to eq 3.

**Table 8. Measured Temperature ( $T$ ), Pressure ( $p$ ), and Density ( $\rho$ ) Data for the 0.66660/0.33340 Molar R-1234yf + R-1234ze(E) Blend<sup>a</sup>**

$T^b$ /K	$p$ /MPa	$\rho$ /kg·m <sup>-3</sup>	$u(p)^c$ /kPa	$100 \cdot (U(\rho)/\rho)^d$	$\Delta\rho^e$
<b>Vapor-phase</b>					
293.149	0.0630	2.989	0.030	0.135	0.000
293.149	0.1234	5.943	0.030	0.077	0.004
293.150	0.1856	9.084	0.030	0.065	0.002
293.150	0.2442	12.136	0.030	0.054	0.000
293.151	0.3014	15.222	0.030	0.051	-0.001
293.154	0.3596	18.471	0.030	0.047	-0.002
293.153	0.4200	21.977	0.030	0.047	0.001
281.157	0.0508	2.512	0.030	0.198	-0.005
281.157	0.1027	5.151	0.030	0.098	-0.005
281.157	0.1533	7.806	0.030	0.066	-0.002
281.156	0.2005	10.359	0.030	0.057	-0.001
281.158	0.2515	13.204	0.030	0.056	0.002
281.161	0.3025	16.160	0.030	0.051	0.008
281.160	0.3251	17.506	0.030	0.048	0.012
273.155	0.0564	2.879	0.030	0.176	-0.024
273.155	0.0900	4.640	0.030	0.097	-0.013
273.156	0.1201	6.254	0.030	0.080	-0.009
273.156	0.1595	8.420	0.030	0.064	-0.004
273.155	0.1933	10.320	0.030	0.063	-0.001
273.158	0.2131	11.461	0.030	0.056	0.003
273.153	0.2310	12.503	0.030	0.056	0.005
273.154	0.2511	13.692	0.030	0.052	0.011
263.154	0.0523	2.775	0.030	0.154	-0.028
263.155	0.0770	4.120	0.030	0.107	-0.017
263.155	0.1069	5.786	0.030	0.087	-0.007
263.154	0.1207	6.567	0.030	0.075	-0.005
263.152	0.1401	7.678	0.030	0.068	-0.001
263.152	0.1637	9.054	0.030	0.064	0.004
263.151	0.1799	10.015	0.030	0.059	0.012
253.155	0.0368	2.019	0.030	0.216	-0.051
253.152	0.0614	3.408	0.030	0.132	-0.030
253.152	0.0842	4.714	0.030	0.103	-0.018
253.152	0.1051	5.941	0.030	0.082	-0.007
253.154	0.1102	6.246	0.030	0.084	-0.004
253.157	0.1202	6.842	0.030	0.075	0.002
<b>Liquid-phase and supercritical states</b>					
230.014	0.9579	1320.352	1.630	0.045	0.187
230.012	0.9576	1320.359	1.500	0.044	0.187
230.010	0.9584	1320.366	1.670	0.045	0.187
240.008	5.5445	1305.661	1.480	0.044	0.188
240.011	5.5463	1305.663	1.340	0.044	0.189
240.013	3.9586	1301.686	2.170	0.047	0.195
240.011	2.4591	1297.830	1.400	0.044	0.202
240.010	1.2698	1294.682	4.020	0.057	0.207

250.004	9.6756	1290.781	1.790	0.045	0.191
250.006	8.0611	1286.603	1.340	0.043	0.197
250.004	5.0435	1278.444	1.660	0.044	0.209
250.007	2.3031	1270.555	1.400	0.044	0.222
250.007	1.2492	1267.385	2.260	0.047	0.227
260.000	9.0428	1263.765	1.520	0.044	0.212
260.001	7.6044	1259.563	1.210	0.043	0.218
260.004	6.2284	1255.416	1.370	0.043	0.224
260.002	2.4584	1243.330	1.860	0.045	0.242
260.003	1.3290	1239.466	1.250	0.043	0.248
269.998	8.5424	1236.121	1.580	0.044	0.233
269.999	7.2639	1231.889	1.380	0.043	0.239
270.001	6.0400	1227.697	1.540	0.044	0.245
269.997	3.7482	1219.475	1.490	0.044	0.258
270.002	1.6599	1211.443	1.280	0.043	0.270
279.999	8.3244	1208.372	1.500	0.044	0.257
280.003	7.1924	1204.103	1.220	0.043	0.263
280.001	5.0621	1195.688	1.300	0.043	0.275
280.004	3.1090	1187.411	1.250	0.043	0.288
280.001	1.3269	1179.339	1.580	0.044	0.300
295.004	10.4177	1175.186	1.340	0.043	0.288
295.003	8.3965	1166.449	1.410	0.043	0.300
295.004	7.4455	1162.109	1.230	0.043	0.306
295.004	5.6600	1153.532	1.250	0.043	0.319
295.005	3.2519	1140.885	1.250	0.043	0.338
295.004	2.5156	1136.726	1.220	0.043	0.345
309.998	10.5000	1132.914	1.340	0.043	0.337
310.002	8.8112	1124.052	1.320	0.043	0.350
310.000	6.5191	1110.918	1.360	0.043	0.372
310.001	4.4982	1097.962	1.230	0.043	0.394
310.004	3.2886	1089.421	1.170	0.043	0.409
310.000	1.6603	1076.765	1.490	0.044	0.431
314.996	3.8770	1075.564	1.360	0.043	0.429
319.993	6.0928	1074.429	1.220	0.043	0.426
324.992	8.3118	1073.367	1.260	0.043	0.421
324.994	7.0982	1064.512	1.350	0.043	0.439
324.994	4.9575	1046.987	1.300	0.043	0.475
324.996	3.5777	1033.973	1.220	0.043	0.503
324.994	1.6531	1012.488	1.450	0.044	0.550
329.990	3.4645	1011.475	1.160	0.043	0.548
334.990	5.2817	1010.507	1.160	0.043	0.541
339.996	7.1044	1009.576	1.100	0.043	0.530
339.998	5.8663	996.239	1.100	0.043	0.566
340.000	5.1261	987.381	1.190	0.043	0.591
339.999	3.5440	965.403	1.210	0.043	0.664
339.999	2.0872	939.260	1.150	0.043	0.776
349.997	4.9568	937.640	1.130	0.043	0.724
360.000	7.8542	936.080	1.140	0.043	0.651
360.002	7.2614	927.025	1.130	0.043	0.686
360.001	5.9881	904.518	1.170	0.043	0.788

360.001	4.9741	882.133	1.090	0.043	0.921
360.001	4.0424	855.376	1.060	0.043	1.140
364.999	5.1398	854.591	1.050	0.043	1.024
369.997	6.2495	853.933	1.080	0.043	0.926
374.999	7.3668	853.267	1.060	0.043	0.839
379.996	8.4859	852.569	1.130	0.044	0.764
379.998	7.5530	829.783	1.090	0.043	0.880
380.001	7.0690	815.792	1.050	0.043	0.964
380.000	6.0518	778.564	1.060	0.044	-3.449
379.999	5.0386	718.366	1.040	0.044	-3.193
380.001	4.2755	602.866	1.050	0.044	-2.307
384.997	4.7733	602.494	1.040	0.044	-2.132
389.997	5.2797	602.121	1.050	0.044	-1.987
394.994	5.7917	601.754	1.050	0.044	-1.864
399.998	6.3087	601.369	1.050	0.044	-1.760
400.002	5.5255	486.234	1.060	0.044	-1.196
400.003	5.0719	394.719	1.070	0.044	-0.817
400.002	4.3633	273.239	1.080	0.051	1.023
400.004	3.8560	213.394	1.090	0.056	0.663
400.002	3.1672	153.911	1.100	0.065	0.356
400.005	2.7375	124.515	1.110	0.075	0.184
400.004	2.2406	95.385	1.110	0.091	0.026
400.005	1.6796	67.018	1.120	0.123	-0.093

---

<sup>a</sup>Reported values are averages of replicate measurements at each  $(T, p)$  state point. <sup>b</sup>Standard uncertainty in temperature is 3 mK. <sup>c</sup>Standard uncertainty in pressure. <sup>d</sup>Relative combined, expanded ( $k = 2$ ) state-point uncertainty in density. <sup>e</sup>Relative deviation from default equation of state calculated according to eq 3.

**Table 9. Relative Deviations of Experimental Data from Values Calculated with Default Mixture Models**

<b>Data Source</b>	<b>AAD<sup>a</sup></b>	<b>MAD<sup>b</sup></b>
<b>R-1234yf + R-134a</b>		
this work	0.240	1.991
Chen et al. <sup>41</sup>	0.375	1.327
Yang et al. <sup>43</sup>	0.393	1.143
Yotsumoto et al. <sup>37</sup>	0.057	0.125
<b>R-134a + R-1234ze(E)</b>		
this work	0.137	0.758
Al Ghafri et al. <sup>38</sup>	0.271	1.073
Zhang et al. <sup>39</sup>	0.339	0.653
<b>R-1234yf + R-1234ze(E)</b>		
this work	0.412	3.774
Al Ghafri et al. <sup>38</sup>	0.467	0.631
Higashi <sup>42</sup>	3.450	23.030

<sup>a</sup>Average absolute deviation calculated according to eq 6. <sup>b</sup>Maximum absolute deviation calculated according to eq 7.

**Table 10. Relative Deviations of Experimental Data from Values Calculated with Updated Mixture Models<sup>22, 40</sup>**

<b>Refrigerant Blend</b>	<b>AAD<sup>a</sup></b>	<b>MAD<sup>b</sup></b>
R-1234yf + R-134a	0.098	0.656
R-134a + R-1234ze(E)	0.034	0.488
R-1234yf + R-1234ze(E)	0.045	0.783

<sup>a</sup>Average absolute deviation calculated according to eq 6. <sup>b</sup>Maximum absolute deviation calculated according to eq 7.

## Figure Captions

**Figure 1.** Molecular representations of refrigerants used in the binary mixtures studied in this work: R-134a, R-1234yf, and R-1234ze(E). Carbon atoms are black, hydrogen atoms are grey, and fluorine atoms are blue. Diagrams were constructed using Avogadro.<sup>44</sup>

**Figure 2.** Measured ( $p$ ,  $\rho$ ,  $T$ ,  $x$ ) state points for three refrigerant blends plotted as density vs temperature. On top are data for two compositions of R-1234yf + R-134a with  $x_1 = 0.33634$  molar shown in (a) and  $x_1 = 0.64709$  molar shown in (b). In the middle are data for two compositions of R-134a + R-1234ze(E) with  $x_1 = 0.33250$  molar shown in (c) and  $x_1 = 0.66356$  molar shown in (d). On bottom are data for two compositions of R-1234yf + R-1234ze(E) with  $x_1 = 0.33584$  molar shown in (e) and  $x_1 = 0.66660$  molar shown in (f). For all graphs:  $\circ$ , measured points; —, phase boundary;  $*$ , critical point. The phase boundaries and critical points were calculated using the default mixture models included in REFPROP (Version 10.0).<sup>24</sup>

**Figure 3.** Relative deviations of the experimental ( $p$ ,  $\rho$ ,  $T$ ,  $x$ ) data for R-1234yf + R-134a from values calculated with REFPROP<sup>24</sup> plotted as a function of (a) temperature, (b) pressure, and (c) density. For all graphs,  $\circ$  represent data for the  $x_1 = 0.33634$  molar blend, while  $\square$  represent data for the  $x_1 = 0.64709$  molar blend. Additionally, black symbols represent vapor-phase data, red symbols represent liquid-phase data, and blue symbols represent data above the critical temperature ( $T_c$ ) with  $T_c = 369.602$  K for the  $x_1 = 0.33634$  molar blend and  $T_c = 367.597$  K for the  $x_1 = 0.64709$  molar blend. Dashed lines are smoothed representations of the overall combined, expanded uncertainty for this binary mixture. Insets show vapor-phase data in greater detail.

**Figure 4.** Relative deviations of the experimental ( $p$ ,  $\rho$ ,  $T$ ,  $x$ ) data for R-134a + R-1234ze(E) from values calculated with REFPROP<sup>24</sup> plotted as a function of (a) temperature, (b) pressure, and

(c) density. For all graphs,  $\circ$  represent data for the  $x_1 = 0.33250$  molar blend, while  $\square$  represent data for the  $x_1 = 0.66356$  molar blend. Additionally, black symbols represent vapor-phase data, red symbols represent liquid-phase data, and blue symbols represent data above the critical temperature ( $T_c$ ) with  $T_c = 378.764$  K for the  $x_1 = 0.33250$  molar blend and  $T_c = 375.866$  K for the  $x_1 = 0.66356$  molar blend. Dashed lines are smoothed representations of the overall combined, expanded uncertainty for this binary mixture. Insets show vapor-phase data in greater detail.

**Figure 5.** Relative deviations of the experimental ( $p, \rho, T, x$ ) data for R-1234yf + R-1234ze(E) from values calculated with REFPROP<sup>24</sup> plotted as a function of (a) temperature, (b) pressure, and (c) density. For all graphs,  $\circ$  represent data for the  $x_1 = 0.33584$  molar blend, while  $\square$  represent data for the  $x_1 = 0.66660$  molar blend. Additionally, black symbols represent vapor-phase data, red symbols represent liquid-phase data, and blue symbols represent data above the critical temperature ( $T_c$ ) with  $T_c = 375.685$  K for the  $x_1 = 0.33584$  molar blend and  $T_c = 370.643$  K for the  $x_1 = 0.66660$  molar blend. Dashed lines are smoothed representations of the overall combined, expanded uncertainty for this binary mixture. Insets show vapor-phase data in greater detail.

**Figure 6.** Relative deviations of experimental density data from values calculated with REFPROP<sup>24</sup> plotted as a function of temperature for (a) R-1234yf + R-134a, (b) R-134a + R-1234ze(E), and (c) R-1234yf + R-1234ze(E). For R-1234yf + R-134a:  $\circ$ , this work ( $x_1 = 0.33634$  molar);  $\square$ , this work ( $x_1 = 0.64709$  molar);  $*$ , Chen et al.<sup>41</sup>;  $\nabla$ , Yang et al.<sup>43</sup>; and  $\triangle$ , Yotsumoto et al.<sup>37</sup>. For R-134a + R-1234ze(E):  $\circ$ , this work ( $x_1 = 0.33250$  molar);  $\square$ , this work ( $x_1 = 0.66356$  molar);  $\triangle$ , Al Ghafri et al.<sup>38</sup> and  $\nabla$ , Zhang et al.<sup>39</sup>. For R-1234yf + R-1234ze(E):  $\circ$ , this work ( $x_1 = 0.33584$  molar);  $\square$ , this work ( $x_1 = 0.66660$  molar); and  $\triangle$ , Al Ghafri et al.<sup>38</sup> and  $\nabla$ , Higashi.<sup>42</sup> Additionally, the light orange shaded region designates the range of corresponding critical temperatures.

**Figure 7.** Relative deviations of experimental density data from values calculated with REFPROP<sup>24</sup> plotted as a function of composition for (a) R-1234yf + R-134a, (b) R-134a + R-1234ze(E), and (c) R-1234yf + R-1234ze(E). For R-1234yf + R-134a: ○, this work ( $x_1 = 0.33634$  molar); □, this work ( $x_1 = 0.64709$  molar); \*, Chen et al.<sup>41</sup>; ▽, Yang et al.<sup>43</sup>; and △, Yotsumoto et al.<sup>37</sup>. For R-134a + R-1234ze(E): ○, this work ( $x_1 = 0.33250$  molar); □, this work ( $x_1 = 0.66356$  molar); △, Al Ghafri et al.<sup>38</sup> and ▽, Zhang et al.<sup>39</sup>. For R-1234yf + R-1234ze(E): ○, this work ( $x_1 = 0.33584$  molar); □, this work ( $x_1 = 0.66660$  molar); and △, Al Ghafri et al.<sup>38</sup> and ▽, Higashi.<sup>42</sup>

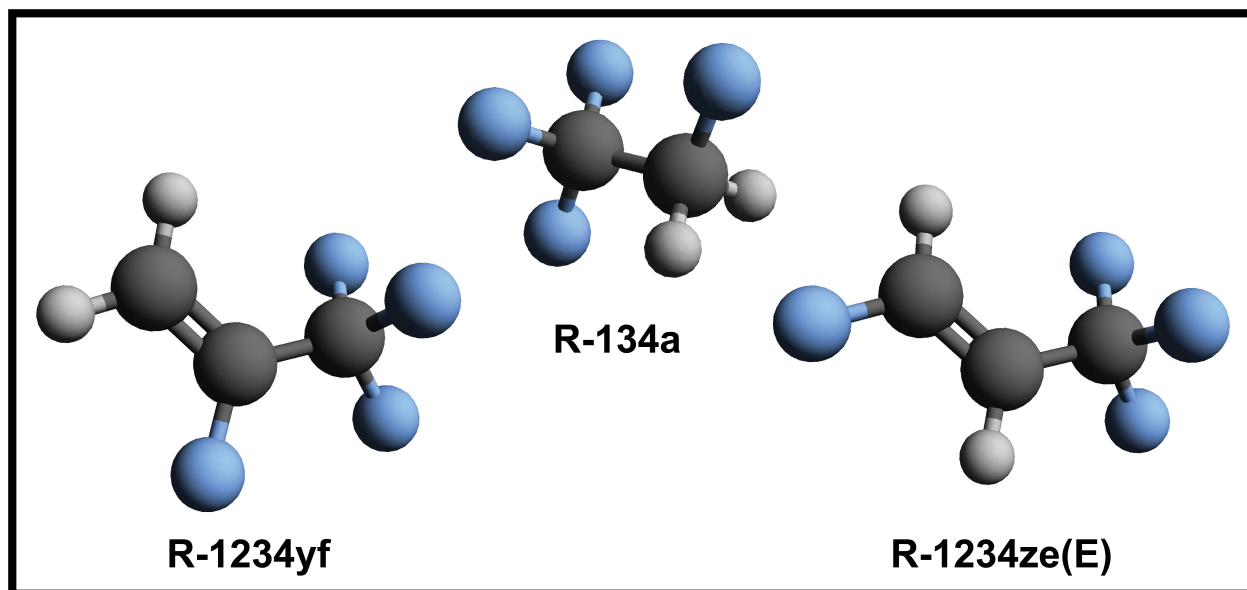


**Figure 1.** Molecular representations of refrigerants used in the binary mixtures studied in this work: R-134a, R-1234yf, and R-1234ze(E). Carbon atoms are black, hydrogen atoms are grey, and fluorine atoms are blue. Diagrams were constructed using Avogadro.<sup>44</sup>

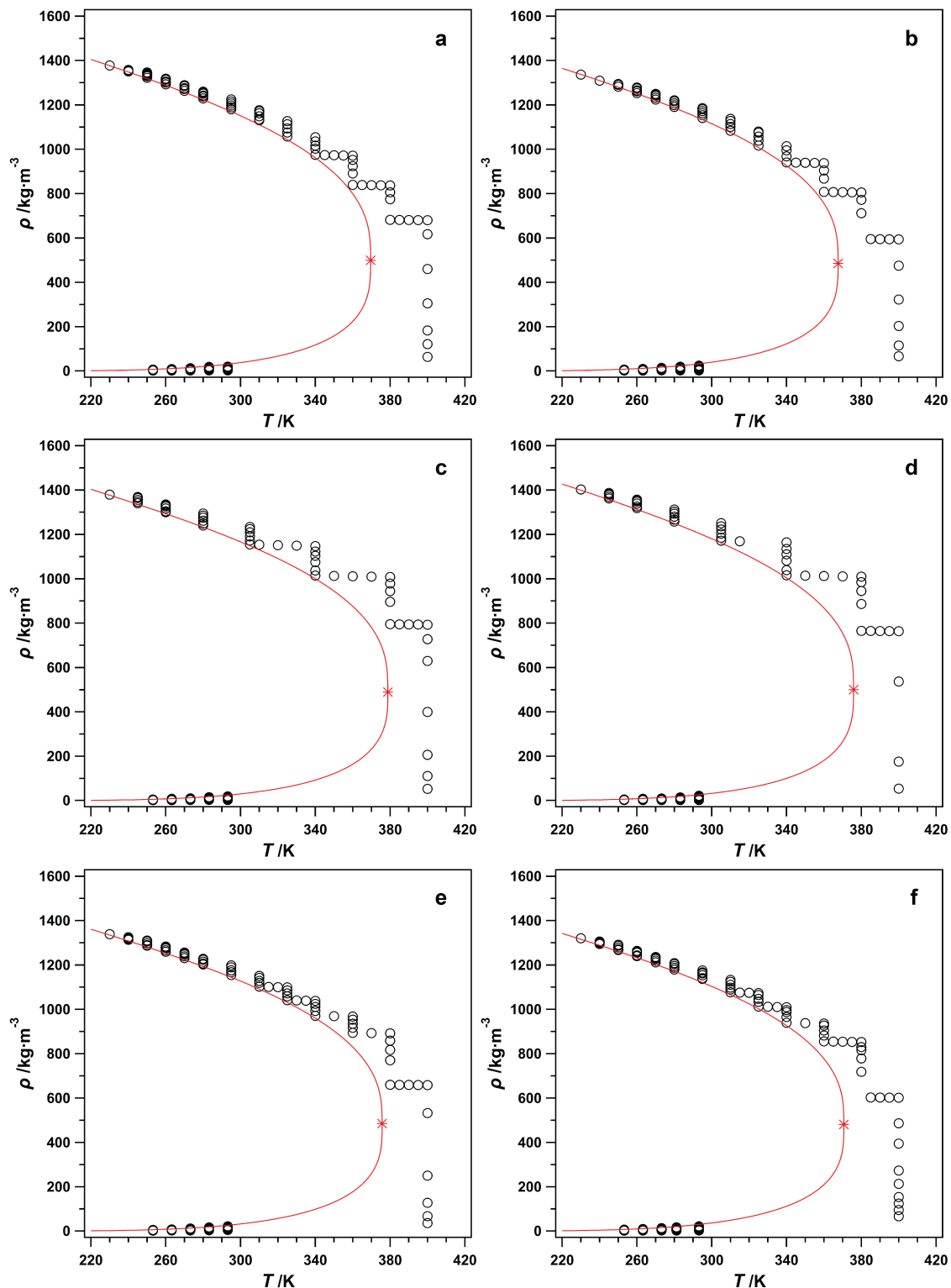


**Figure 2.** Measured  $(p, \rho, T, x)$  state points for three refrigerant blends plotted as density vs temperature. On top are data for two compositions of R-1234yf + R-134a with  $x_1 = 0.33634$  molar shown in (a) and  $x_1 = 0.64709$  molar shown in (b). In the middle are data for two compositions of R-134a + R-1234ze(E) with  $x_1 = 0.33250$  molar shown in (c) and  $x_1 = 0.66356$

molar shown in (d). On bottom are data for two compositions of R-1234yf + R-1234ze(E) with  $x_1 = 0.33584$  molar shown in (e) and  $x_1 = 0.66660$  molar shown in (f). For all graphs:  $\circ$ , measured points; —, phase boundary;  $*$ , critical point. The phase boundaries and critical points were calculated using the default mixture models included in REFPROP (Version 10.0).<sup>24</sup>

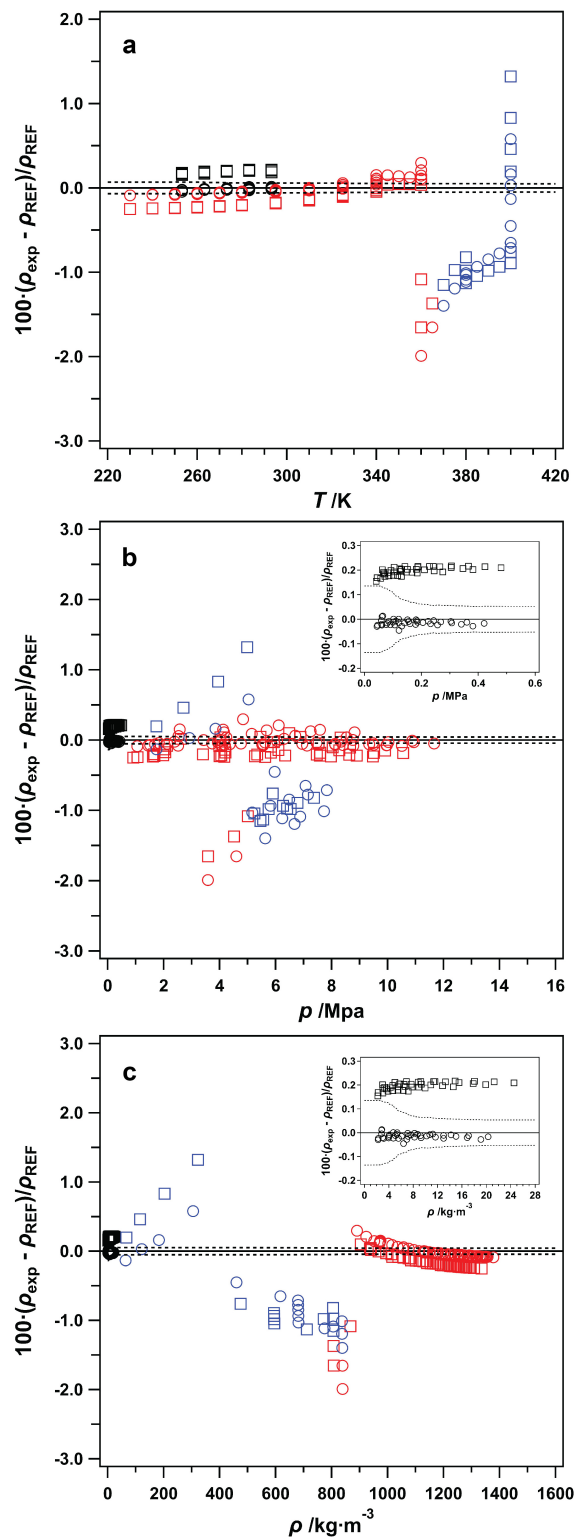


**Figure 3.** Relative deviations of the experimental ( $p$ ,  $\rho$ ,  $T$ ,  $x$ ) data for R-1234yf + R-134a from values calculated with REFPROP<sup>24</sup> plotted as a function of (a) temperature, (b) pressure, and (c) density. For all graphs,  $\circ$  represent data for the  $x_1 = 0.33634$  molar blend, while  $\square$  represent data for the  $x_1 = 0.64709$  molar blend. Additionally, black symbols represent vapor-phase data,

red symbols represent liquid-phase data, and blue symbols represent data above the critical temperature ( $T_c$ ) with  $T_c = 369.602$  K for the  $x_1 = 0.33634$  molar blend and  $T_c = 367.597$  K for the  $x_1 = 0.64709$  molar blend. Dashed lines are smoothed representations of the overall combined, expanded uncertainty for this binary mixture. Insets show vapor-phase data in greater detail.

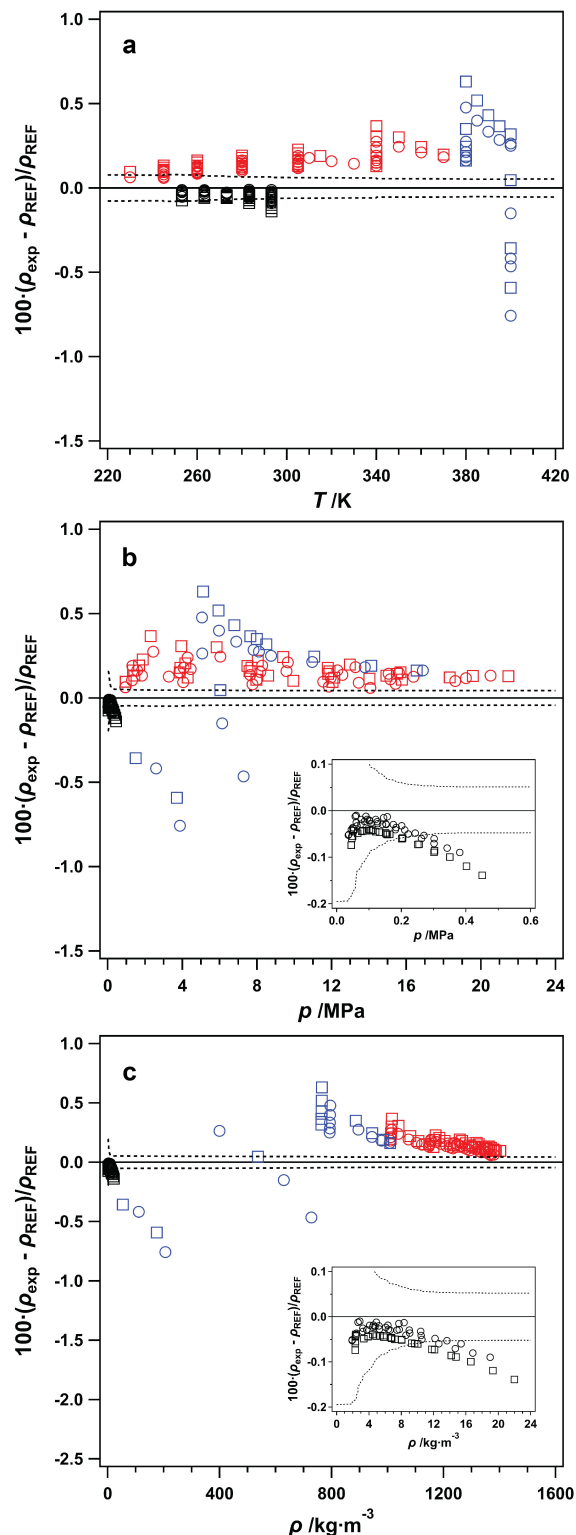


**Figure 4.** Relative deviations of the experimental ( $p$ ,  $\rho$ ,  $T$ ,  $x$ ) data for R-134a + R-1234ze(E) from values calculated with REFPROP<sup>24</sup> plotted as a function of (a) temperature, (b) pressure, and (c) density. For all graphs,  $\circ$  represent data for the  $x_1 = 0.33250$  molar blend, while  $\square$  represent data for the  $x_1 = 0.66356$  molar blend. Additionally, black symbols represent vapor-

phase data, red symbols represent liquid-phase data, and blue symbols represent data above the critical temperature ( $T_c$ ) with  $T_c = 378.764$  K for the  $x_1 = 0.33250$  molar blend and  $T_c = 375.866$  K for the  $x_1 = 0.66356$  molar blend. Dashed lines are smoothed representations of the overall combined, expanded uncertainty for this binary mixture. Insets show vapor-phase data in greater detail.

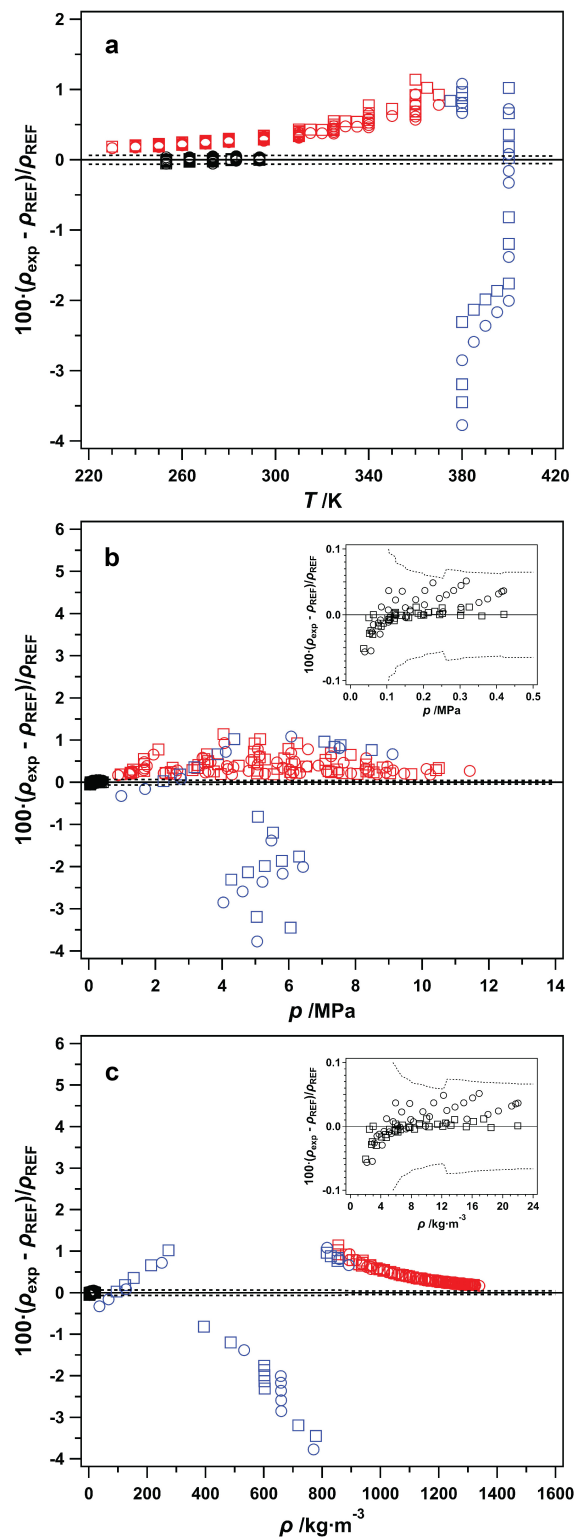


**Figure 5.** Relative deviations of the experimental ( $p$ ,  $\rho$ ,  $T$ ,  $x$ ) data for R-1234yf + R-1234ze(E) from values calculated with REFPROP<sup>24</sup> plotted as a function of (a) temperature, (b) pressure, and (c) density. For all graphs,  $\circ$  represent data for the  $x_1 = 0.33584$  molar blend, while  $\square$  represent data for the  $x_1 = 0.66660$  molar blend. Additionally, black symbols represent vapor-

phase data, red symbols represent liquid-phase data, and blue symbols represent data above the critical temperature ( $T_c$ ) with  $T_c = 375.685$  K for the  $x_1 = 0.33584$  molar blend and  $T_c = 370.643$  K for the  $x_1 = 0.66660$  molar blend. Dashed lines are smoothed representations of the overall combined, expanded uncertainty for this binary mixture. Insets show vapor-phase data in greater detail.

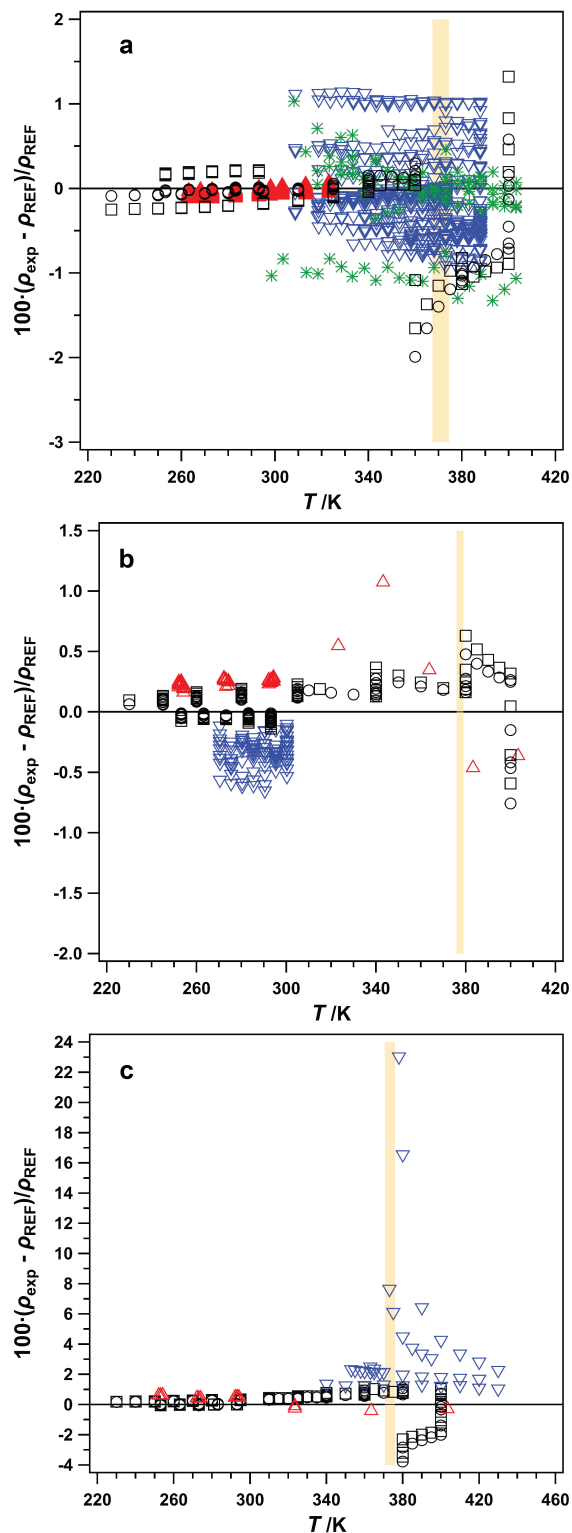


**Figure 6.** Relative deviations of experimental density data from values calculated with REFPROP<sup>24</sup> plotted as a function of temperature for (a) R-1234yf + R-134a, (b) R-134a + R-1234ze(E), and (c) R-1234yf + R-1234ze(E). For R-1234yf + R-134a: ○, this work ( $x_1 = 0.33634$  molar); □, this work ( $x_1 = 0.64709$  molar); \*, Chen et al.<sup>41</sup>; ▽, Yang et al.<sup>43</sup>; and △,

Yotsumoto et al.<sup>37</sup>. For R-134a + R-1234ze(E): ○, this work ( $x_1 = 0.33250$  molar); □, this work ( $x_1 = 0.66356$  molar); △, Al Ghafri et al.<sup>38</sup> and ▽, Zhang et al.<sup>39</sup>. For R-1234yf + R-1234ze(E): ○, this work ( $x_1 = 0.33584$  molar); □, this work ( $x_1 = 0.66660$  molar); and △, Al Ghafri et al.<sup>38</sup> and ▽, Higashi.<sup>42</sup> Additionally, the light orange shaded region designates the range of corresponding critical temperatures. Where needed, the graph region covering the majority of data points has been expanded and is shown in the inset for clarity.

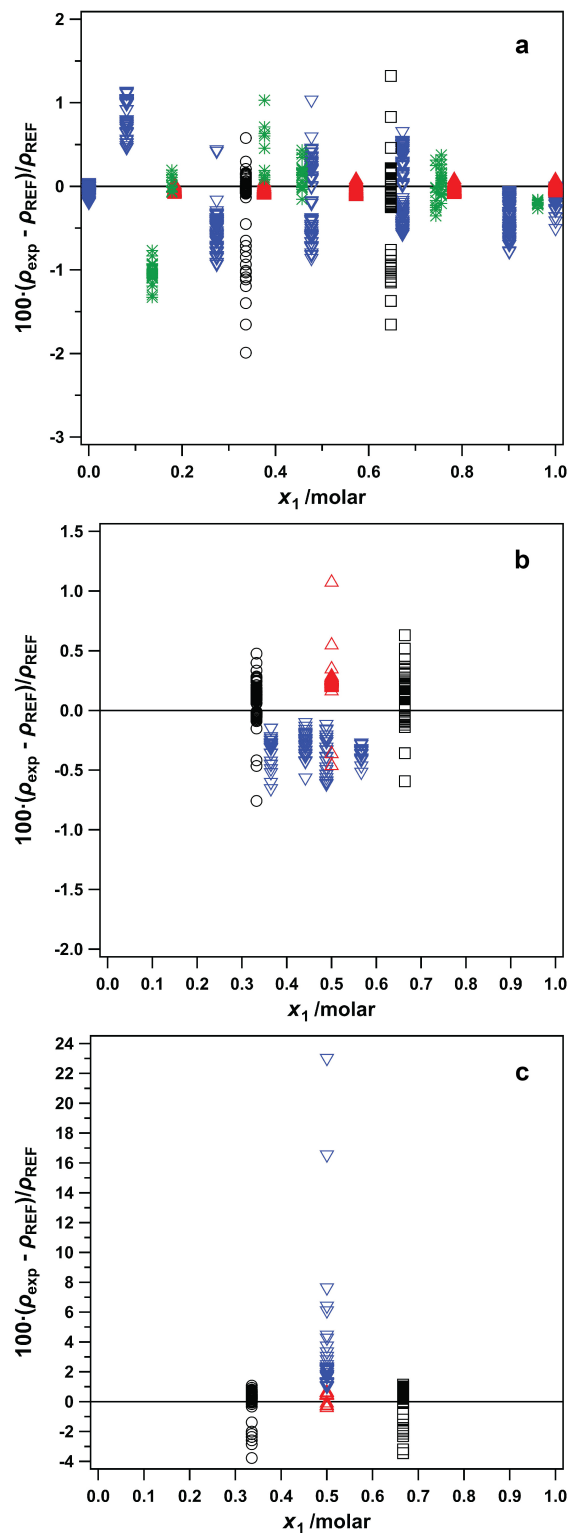


**Figure 7.** Relative deviations of experimental density data from values calculated with REFPROP<sup>24</sup> plotted as a function of composition for (a) R-1234yf + R-134a, (b) R-134a + R-1234ze(E), and (c) R-1234yf + R-1234ze(E). For R-1234yf + R-134a: ○, this work ( $x_1 = 0.33634$  molar); □, this work ( $x_1 = 0.64709$  molar); \*, Chen et al.<sup>41</sup>; ▽, Yang et al.<sup>43</sup>; and △,

Yotsumoto et al.<sup>37</sup>. For R-134a + R-1234ze(E): ○, this work ( $x_1 = 0.33250$  molar); □, this work ( $x_1 = 0.66356$  molar); △, Al Ghafri et al.<sup>38</sup> and ▽, Zhang et al.<sup>39</sup>. For R-1234yf + R-1234ze(E): ○, this work ( $x_1 = 0.33584$  molar); □, this work ( $x_1 = 0.66660$  molar); and △, Al Ghafri et al.<sup>38</sup> and ▽, Higashi.<sup>42</sup> Where needed, the graph region covering the majority of data points has been expanded and is shown in the inset for clarity.